Performance and Transient Behaviour of *MGT* Based Energy Systems

R. Tuccillo
Dipartimento di Ingegneria Meccanica per l'Energetica (D.I.M.E.)
Università di Napoli "Federico II"
via Claudio 21
80125 Napoli
ITALY

tuccillo@unina.it

ABSTRACT

After a preliminary overview of the multiplicity of solutions for the set up and operation of energy conversion systems based on micro-gas turbines, this paper outlines the method for performance evaluation under both steady state and transient conditions. The cycle analysis aims at the evaluation of thermal efficiency and energy saving indices under different fuelling conditions and with variably recuperated cycle. The subsequent component matching simulation extends the MGT analysis to the off-design conditions and it leads to the definition of methods for an efficient fulfilment of variable external loads. Finally, the study of some typical transient developments, of both the full-to-part and the part-to-full load type, introduces to the problem of defining proper fuel control laws as to prevent excesses in both energy consumption and component stresses and instabilities.

1. FOREWORDS

The micro-gas turbine based energy conversion systems represent one of the most recently developed devices for power generation also for cogeneration application. The set up of an efficient *MGT* based power plant usually exploits the well established manufacturers' experience in the field of industrial gas turbines but also requires specifically studies to be addressed to the specific problems involving the small-scale devices. Therefore, this lecture starts with the state of art of the existing microturbines and of the different approaches followed by several researchers and manufacturers, say:

- The manufacturing and testing of devices on a real micro-scale with the related technology advancements, in terms of design concepts and silicon based materials;
- The component selection or design, the latter based on truly innovative concepts or on the scaling of radial flow turbomachines;
- The MGT bases plants integrated with the gasification systems of bio-masses or solid wastes;
- The thermo-economic analysis of MGT power systems for cogeneration of tri-generation purposes.

It is beyond the scope of this paper to describe the hybrid systems based on the integration of micro-gas turbines with fuel cells, that are worthy of a separate exhaustive discussion. Therefore the possibility of achieving a competitive performance level with other energy conversion systems of the same power range is strongly dependent on the gas turbine cycle optimisation. The widely employed system is the recuperated cycle and the internal heat exchanger plays a fundamental role in terms of both effectiveness

Tuccillo, R. (2005) Performance and Transient Behaviour of *MGT* Based Energy Systems. In *Micro Gas Turbines* (pp. 6-1 – 6-56). Educational Notes RTO-EN-AVT-131, Paper 6. Neuilly-sur-Seine, France: RTO. Available from: http://www.rto.nato.int/abstracts.asp.

and reduced size. So this article extensively describes the manufacturers' experience in this field and analyses the possibilities of an efficient management of the recuperated micro-gas turbine. Really, many authors have conceived the partly recuperated cycle as a tool for adapting the MGT output to variable electricity and heat requirements.

Basing on the above items the paper proceeds, after the preliminary overview, with the cycle analysis of micro-gas turbines supplied with different fuels and with the partial by-pass of the recuperator. After that, a method for the performance estimation is introduced in order to identify the main degrees of freedom of the MGT based plant and to outline the optimal strategies for fulfilling variable electrical and thermal loads.

The final section of the paper is dedicated to examples of MGT transients. Such phenomena are of particular interest since the unsteady transition between two different regimes involves remarkable changes in the component operation and in particular for the combustor and the heat exchangers. Consequently an inappropriate control of the transient development may lead to undesired increases in both fuel consumption and pollutant production. To this purpose, the effect of different fuel control laws are compared.

2. STATE OF THE ART

The rising growth of researches on the several subjects concerning the micro-gas turbines confirms the interest towards the low-range energy conversion systems, whose attractiveness and competitiveness can be enhanced by both satisfactory energetic performance and low-cost manufacturing. Therefore the technical literature is plentiful of articles focusing the attention on the MGT based power plants and on its components, not only under the thermo-fluid-dynamic point of view but also by addressing the interest to the material technology and to the economic aspects as well.

The well established goal of obtaining acceptable performance levels without exceeding in the cost of the most critical components constrains the choice of the thermal cycle within limits for both pressure ratios and firing temperatures: Consequently the cycle options which can be accounted for must make an almost mandatory use of the internal heat recovery. The well known overview in ref. [44] (fig. 2.1) outlines a variety of possibilities for the thermal cycle, both of the open and of the semi-closed type, but all of these include the recuperator as a key component for achieving acceptable efficiency levels.

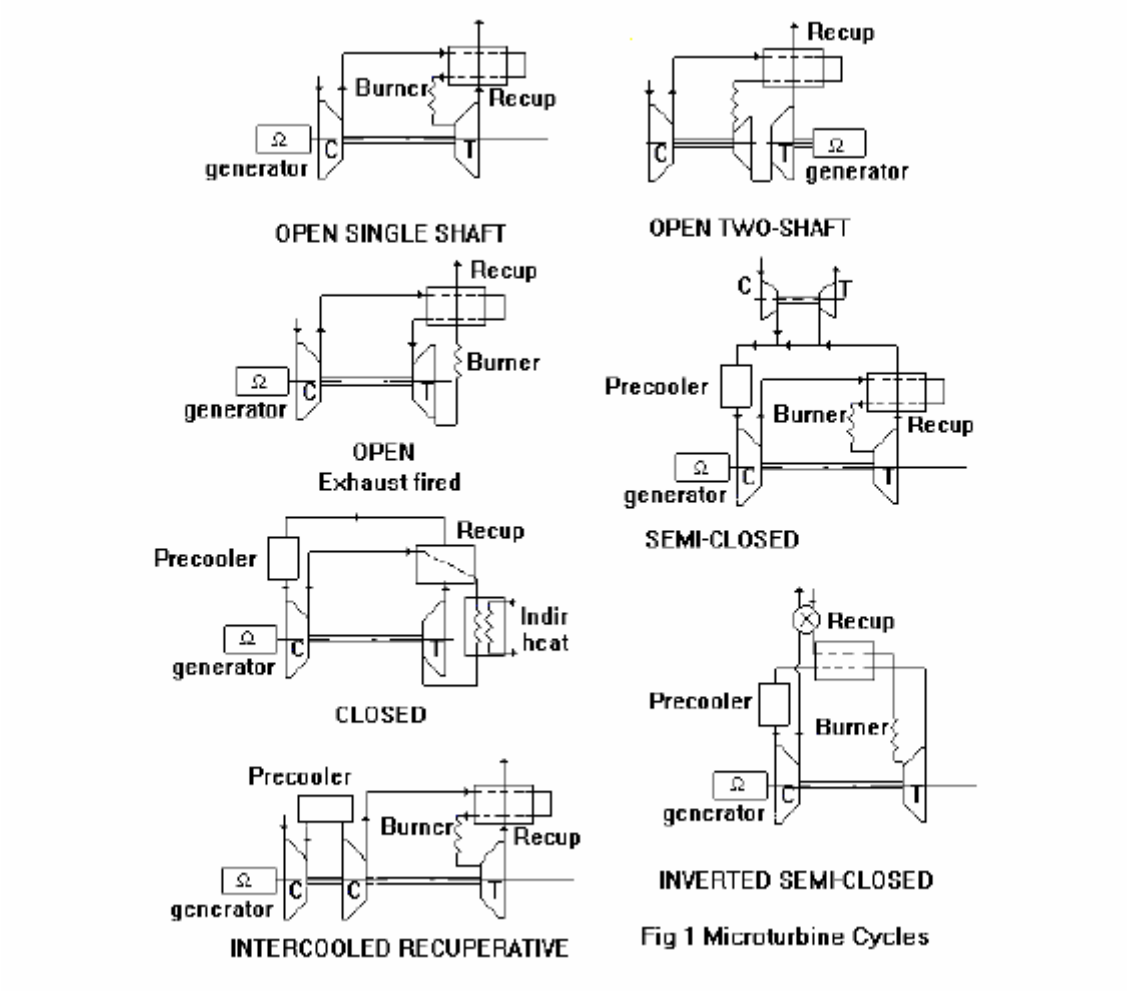

Figure 2.1: Overview of the Cycle Options for Micro-Gas Turbines (from ref. [44]).

The central role played by the recuperator is emphasized by diagrams like that in figure 2.2 [18], which underlines the importance of both the heat recovery efficiency and the pressure losses on the cycle efficiency. The same figure evidences that the specific cost of this component is significantly higher when dealing with low range gas-turbines with turbine inlet temperatures of (900 – 1100 °C). Thus, obtaining the most effective recuperated cycle without increasing the size and the weight of this component is the straightest way for achieving a real thermo-economic competitiveness of the micro-gas turbine.

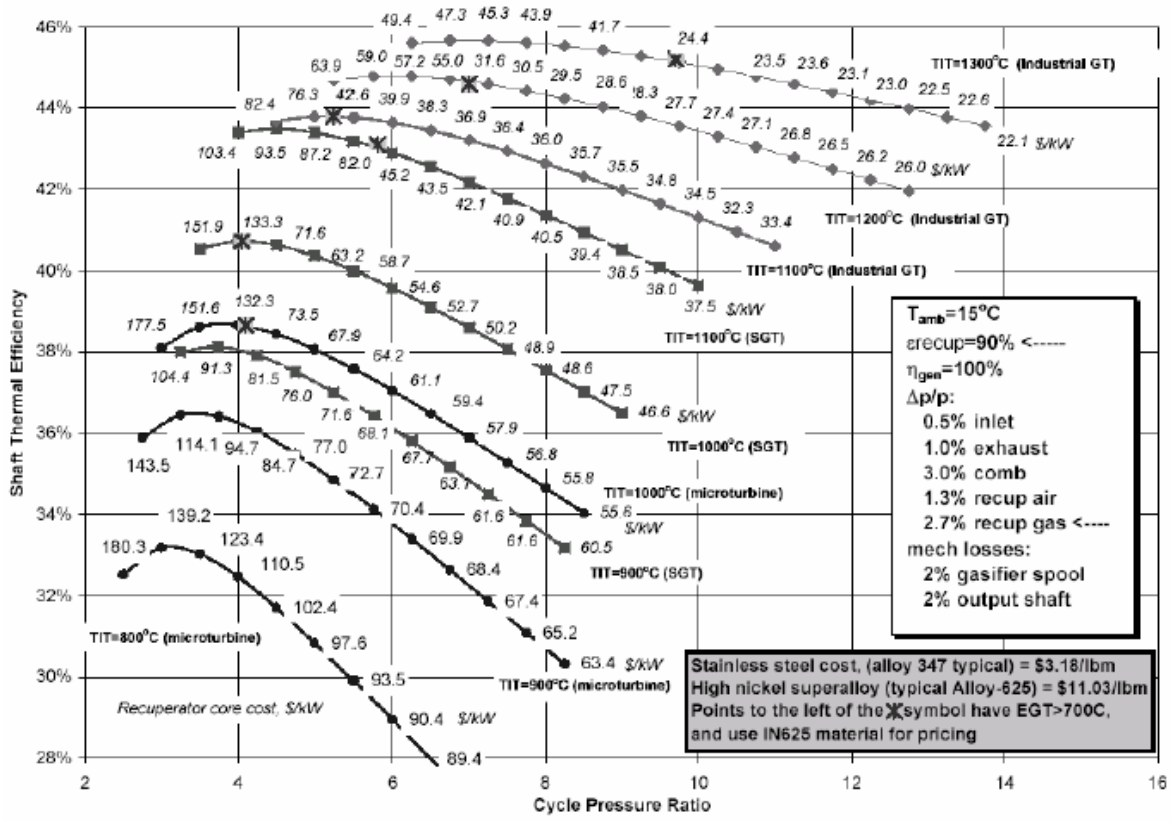

Figure 2.2: Thermal Efficiency and Specific Costs of the Recuperator (from ref. [18]).

The above considerations clearly explain the interest that many industrial and academic researchers have paid to several topics involving the recuperator technology [1-18]. Since many years, Mc Donald [1-5] addressed his studies to the advancements in recuperator technology and in more recent years the interest has been specifically focused on the small gas turbines area, so proposing a low cost recuperator concept [5], like the one displayed in fig. 2.3.

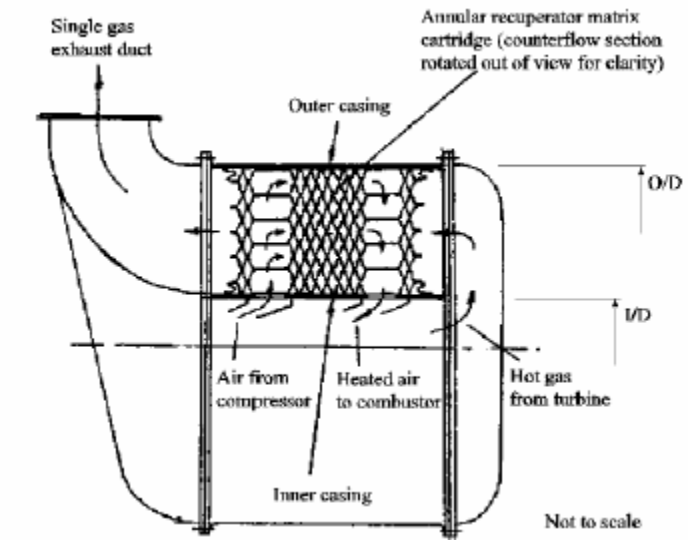

Figure 2.3: Annular, Low-Cost Recuperator Cost (from ref. [5]).

Different recuperator concepts have been proposed and introduced in recent years and some examples are displayed in figures 2.4 to 2.8, starting from those of the annular type in fig. 2.4 [15], and proceeding with the counter flow recuperators [10, 18] in figs. 2.5 and 2.6, till to the spiral configurations [12] and the concentric tube arrangement [13] in figures 2.7 and 2.8 respectively. Such examples demonstrate the actual interest of many manufacturers in the field of compact and efficient recuperators for micro-gas turbine applications.

Figure 2.4: Annular Recuperator for a 200 kW MGT (from ref. [15]).

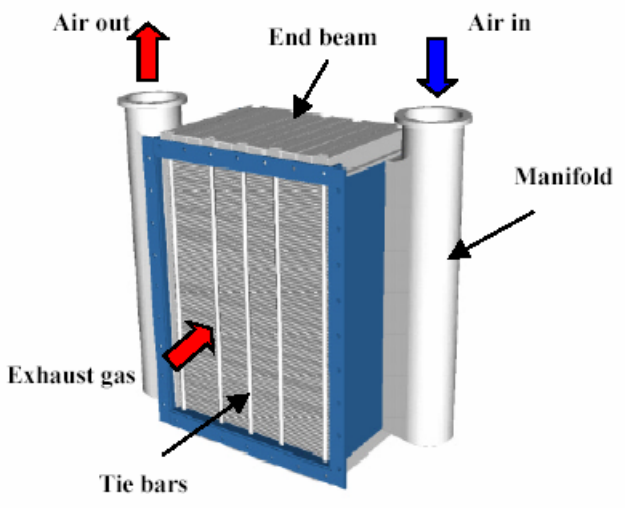

Figure 2.5: A Counter Flow Recuperator (from ref. [10]).

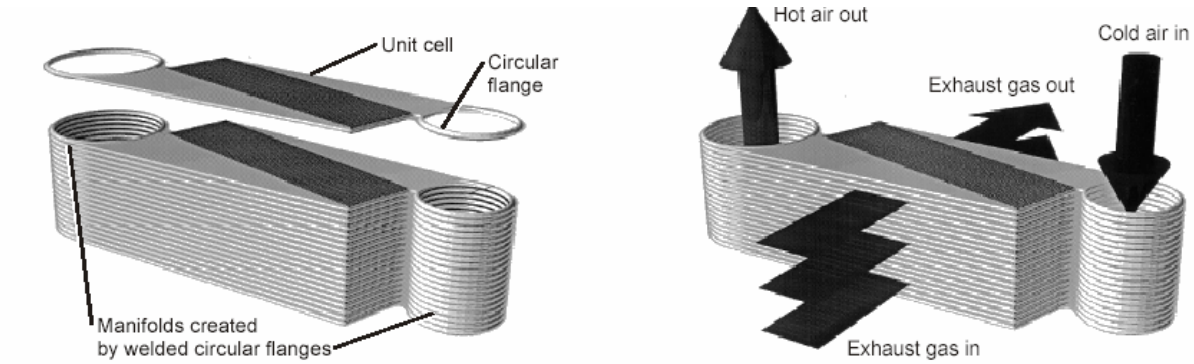

Figure 2.6: Core Fabrication and Flow Path in a Counter Flow Recuperator (from ref. [18]).

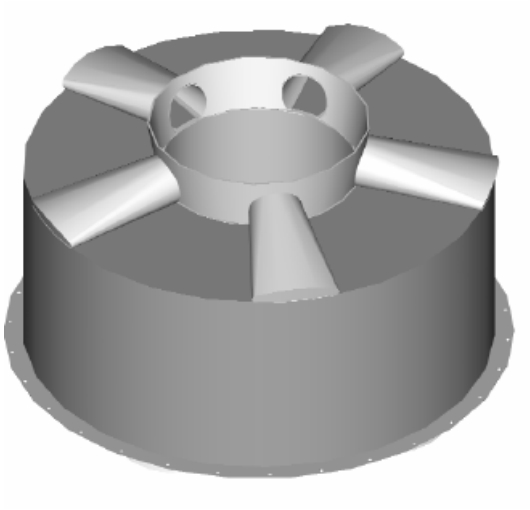

Figure 2.7: CAD Sketch of a Spiral Recuperator (from ref. [12]).

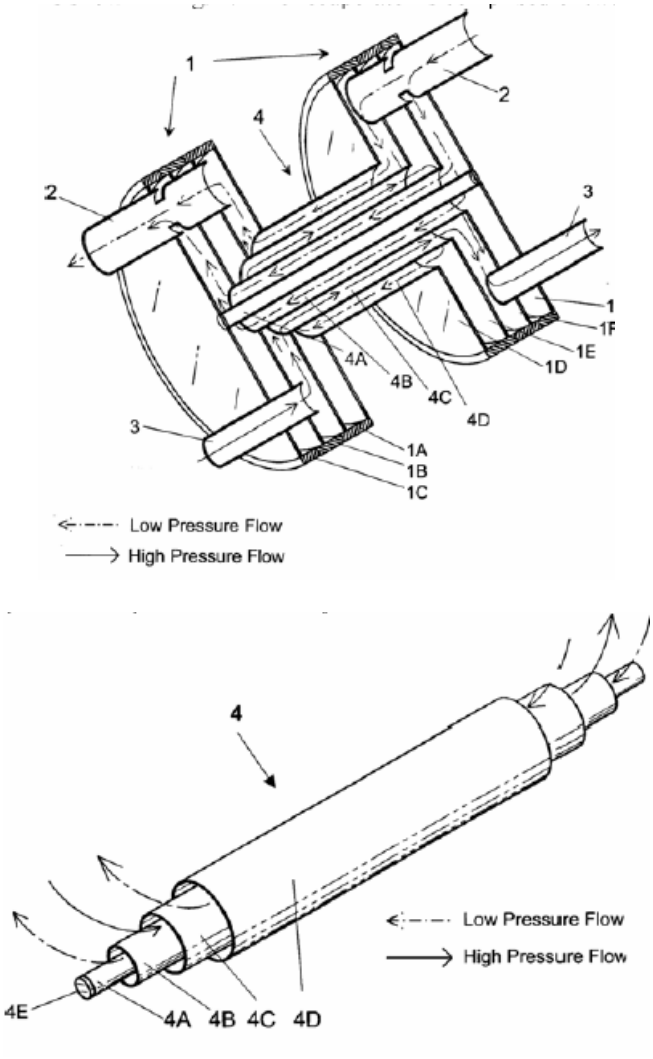

Figure 2.8: The Concentric Flow Recuperator (from ref. [12]).

The importance of the heat exchangers as tools for improving the thermal cycle efficiency of microturbines is confirmed by a number of proposals of advanced cycles for MGTs like the intercooled and recuperated cycle in [11] (fig. 2.9) and the reheat cycle proposed in refs. [14, 67] (fig. 2.10). In the first paper a fundamental role is also played by the whole plant arrangement and by the external intercooler compactness.

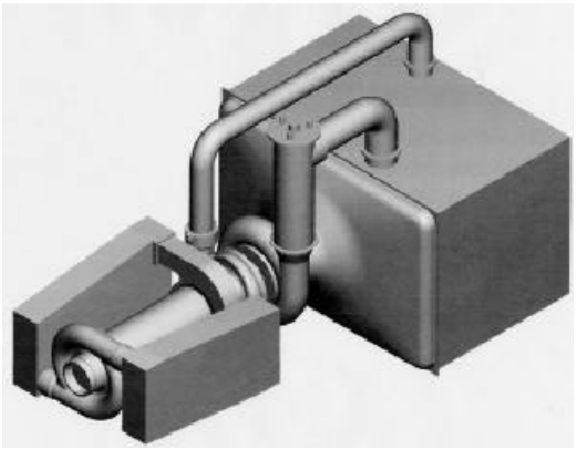

Figure 2.9: Schematics of Intercooled and Recuperated MGT (from ref. [11]).

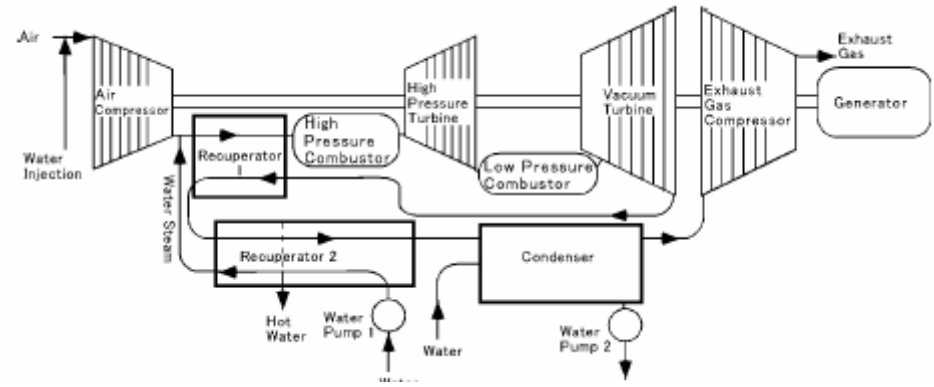

Figure 2.10: Recuperated – Reheat MGT with Humid Air Cycle (from ref. [14, 67]).

The second includes two recuperating heat exchanger operating within a humid air cycle. This proposal can be found also in other authors and will be discussed in the following as an effective option for both enhancing the cycle efficiency and stabilizing the microturbine performance under variable inlet air conditions. In papers [14, 67] the humid air solution implies the use of two recuperators, the second one expressly addressed to the water evaporation, and of the condenser for the recovery of the water injected.

The need for an efficient response of the recuperating heat exchanger under a wide variety of operating conditions also results in attempts to define the optimal configuration of this components. An example can be found in ref. [17], together with an off-design analysis (fig. 2.11).

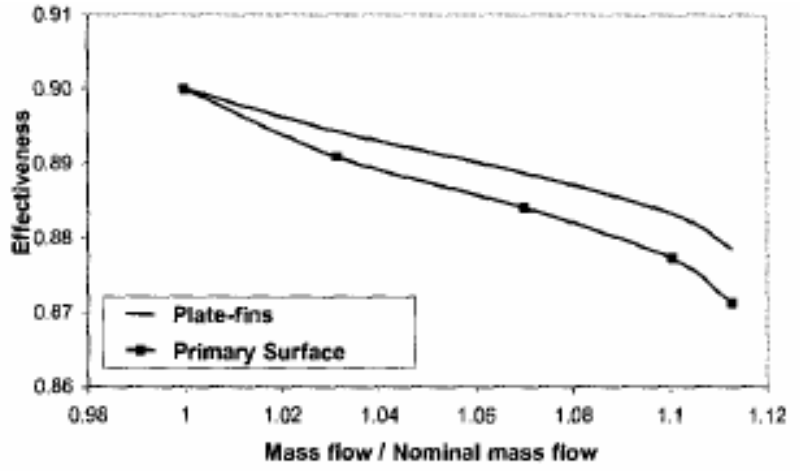

Figure 2.11: Recuperator Off-Design Curves (from ref. [17]).

Finally, the studies on the recuperators are also extended to the material response in terms of creep resistance [6, 7, 8]. The diagram in figure 2.12 refers to a typical operating temperature of this device and it clearly shows that a non-proper choice of the materials may lead to a rapid failure due to an excess in creep strain.

The researches on the materials for the micro-gas turbine components represent an interesting field specially for identifying the possibilities of operating without cooling systems. Both ceramic and silicon based materials are therefore widely investigated [19-24], the latter mainly for the manufacturing of truly miniaturized components, as discussed in the following.

The employment of ceramic materials is also foreseen for many components and fig. 2.13 shows in particular the case of vane rings [23].

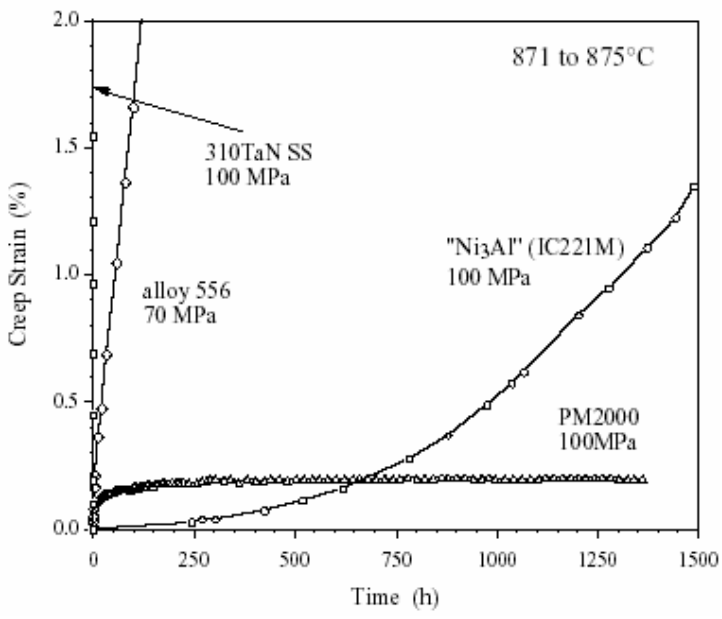

Figure 2.12: Creep-Resistance Diagram of Recuperator Alloys (from ref. [8]).

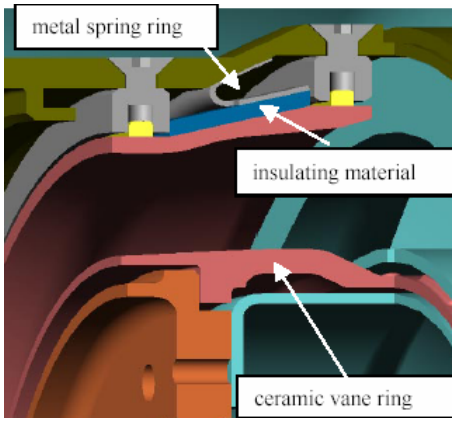

Figure 2.13: Ceramic Materials Employed for Vane Rings (from ref. [23]).

Besides the studies on the MGT materials, an additional field of great interest is the one related to the adoption of alternative fuels like those from gasification of solid wastes or bio-masses or other recoverable sources [25, 35]. Two basic topics are the main subjects of investigation, say the adaptation of the MGT combustion system to a different fuelling and the integration of the gasifier with the power plant. Regarding the first subject, an emerging proposal is the use of indirectly fired cycles [31, 34], and some examples in this sense are reported in figures 2.14 and 2.15. Both subjects are exhaustively examined in ref. [33] which analyses the complete integration of a 80 kW micro-gas turbine with the thermal hydrolysis system for the bio-masses. In addition, the same paper pays attention to the variations in plant and combustor behaviour with the fuel characteristics and two control systems are compared, based on constant T.I.T. and constant fuel energy input, respectively. The CFD simulation of the combustion chamber allows prediction of the environmental impact with the different fuel supplies. The plant layout is displayed in fig. 2.16.

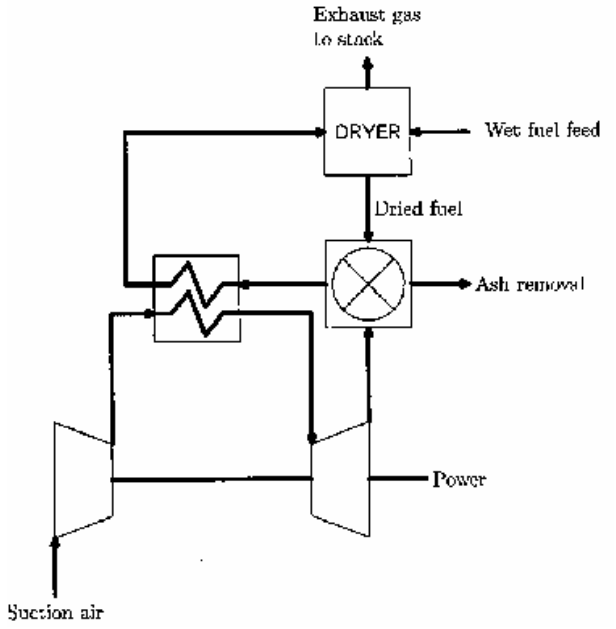

Figure 2.14: Indirectly Fired Gas Turbine with Wet Biomasses (from ref. [31]).

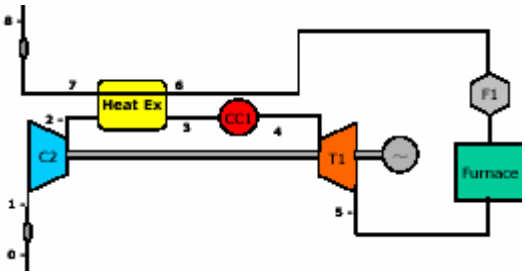

Figure 2.15: The Micro-Gas Turbine with Bio-Furnace (from ref. [34]).

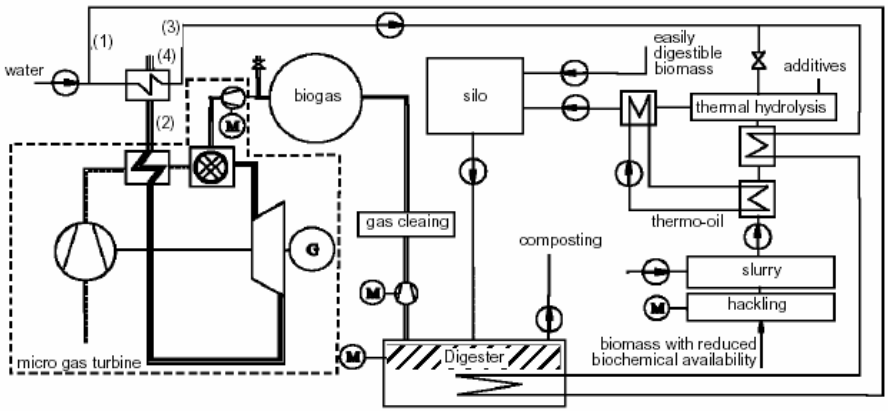

Figure 2.16: Indirectly Fired Gas Turbine with Wet Biomasses (from ref. [33]).

Finally, the authors in ref. [30, 32, 35] comprehensively describe and analyze, also by a thermo-economic point of view, MGT based power and combined plants integrated with systems for the pyrolysis of solid wastes or bio-masses. An example of the proposed layouts is given in fig. 2.17.

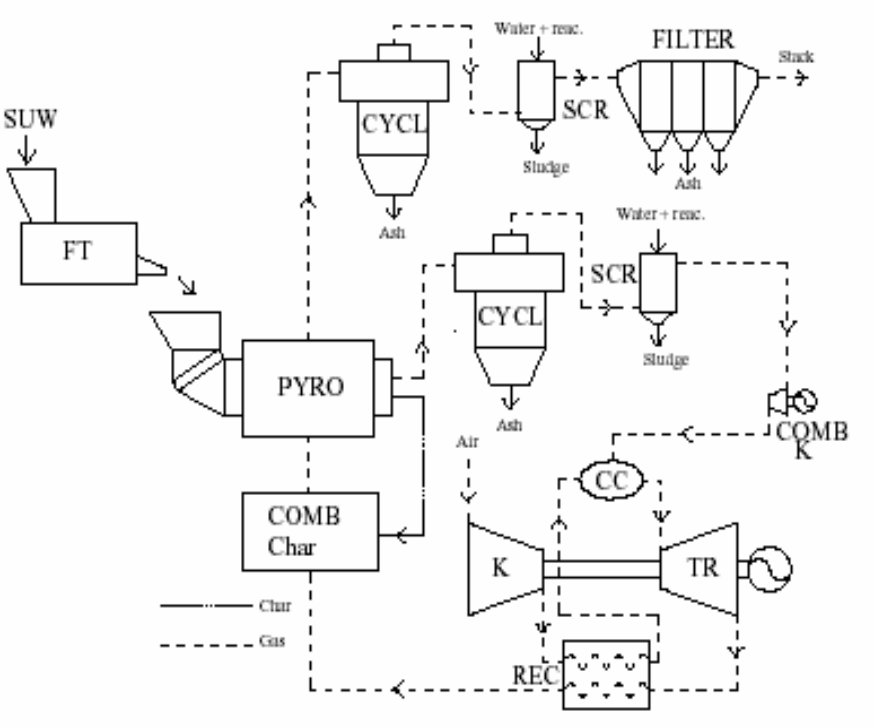

Figure 2.17: A Proposal of Integrated Plant with Micro-Gas Turbine and Solid-Waste Pyrolysis System (from ref. [30]).

The studies on the microturbine prototypes [36-41, 88] aim at demonstrating that the future development of the micro-gas turbine could happen on a real micro-scale basis. In this field, the leading studies are those carried out at the MIT on silicon based combustion systems [37, 38, 39] with prototypes of a few millimetre diameter and extreme rotational speeds (of the order of magnitude of 10^6 rpm). The well known radial arrangement which has been proposed in [37], (fig. 2.18) also confirms that the technology development in this field may lead to thermal power density higher than those of the most advanced heavy duty gas turbines. Similar studies on the feasibility of a micro-scale gas turbines are described in ref. [36] that proposes a fully 2D impeller (fig. 2.19).

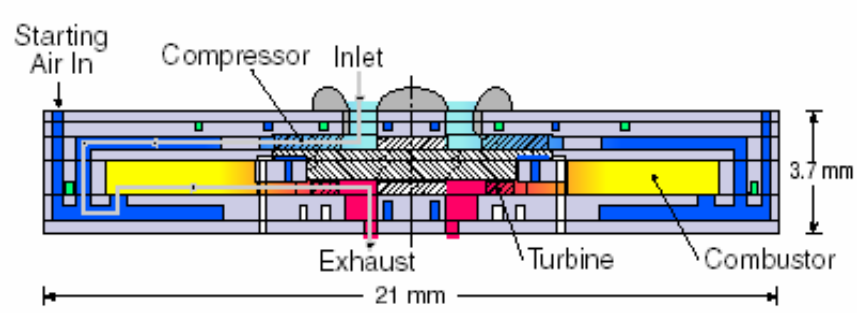

Figure 2.18: The Silicon-Based, High Power Density Gas Turbine (from ref. [37]).

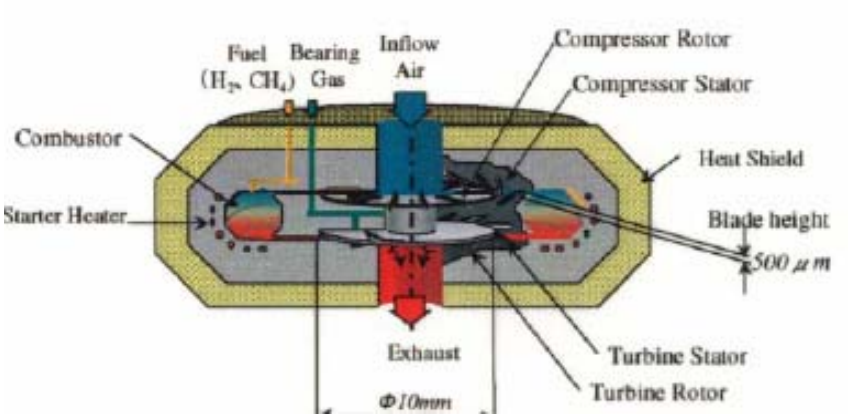

Figure 2.19: The Micro-Scale Gas Turbine with 2D Impeller (from ref. [36]).

Specific studies on the rotating components are presented in ref. [39, 40, 41]. The first paper deals with the manufacturing and testing of radial compressors and turbine expressly conceived for an arrangement similar to the one in fig. 2.18. Therefore, both compressor and turbine are designed for a planar radial flow (fig. 2.20)

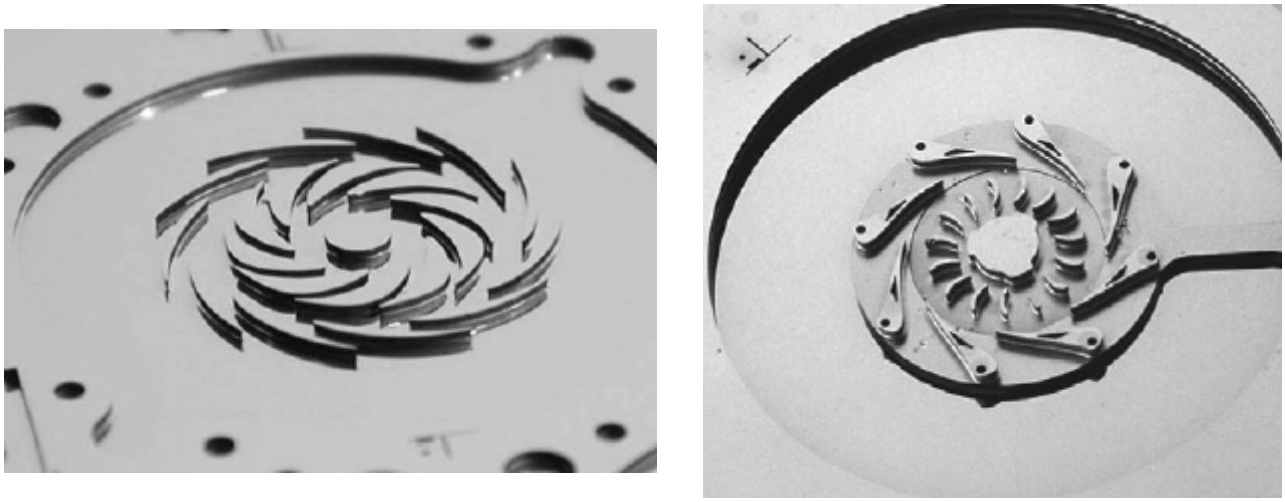

Figure 2.20: Centrifugal Flow Compressor and Radial Inflow Turbine on Micro-Scale (from ref. [39]).

A rather different approach is followed by the authors of paper [40], whose interest is addressed to the study of a typical mixed flow impeller geometry reduced to a micro-scale size (fig. 2.21). Similarly the centripetal flow turbine is obtained by scaling a conventional geometry (fig. 2.21). Such a method introduces a fundamental problem which arises when dealing with the fluid-dynamics of micro-scaled turbomachines. Really, operating with extremely reduced sizes implies low Reynolds flows so that the laminar or transitional regimes may occur. In addition, the blade surface roughness effect is amplified and the resulting cascade loss coefficients may dramatically increase (fig. 2.22).

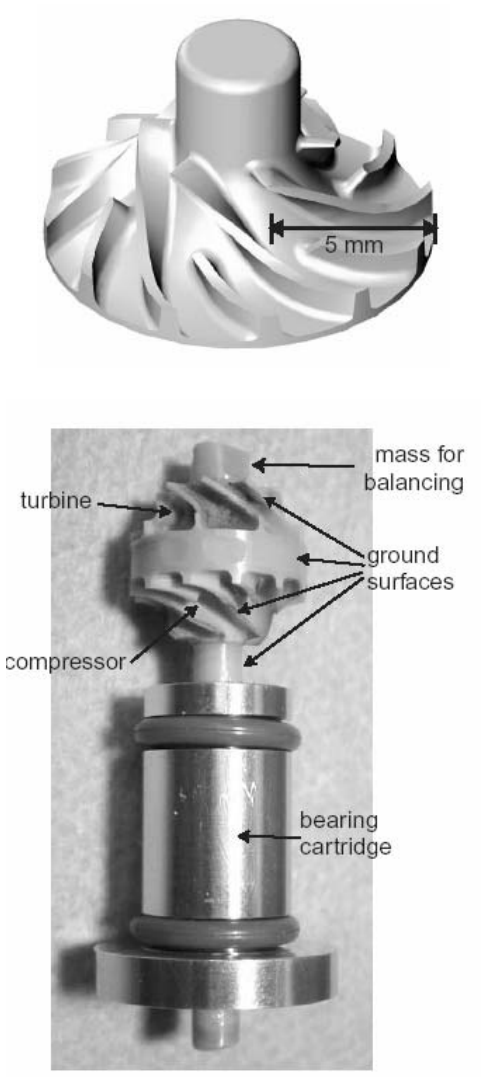

Figure 2.21: Micro-Scaled Rotating Components and Shaft Assembly (from ref. [40]).

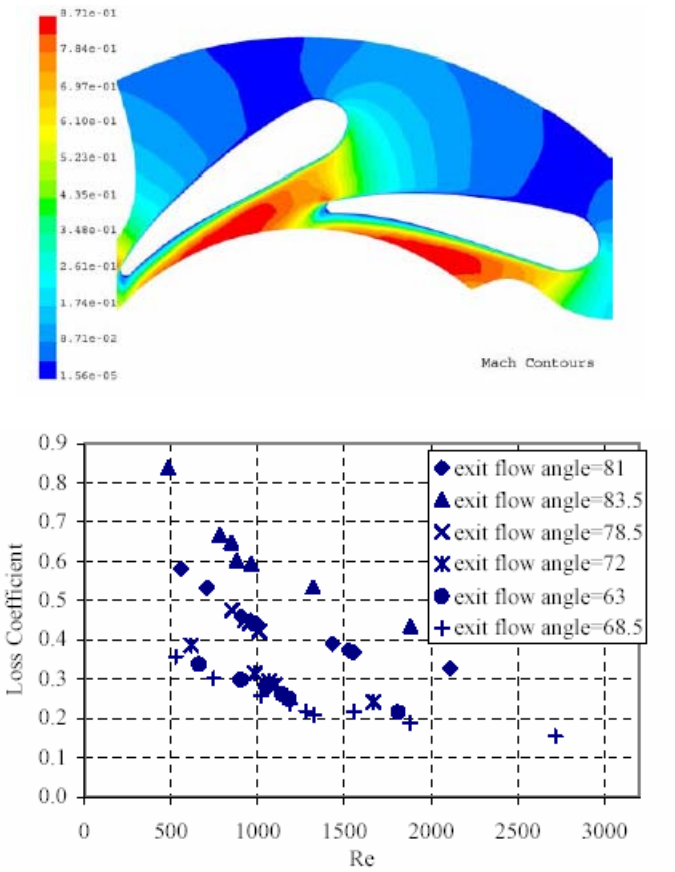

Figure 2.22: Mach Number Contours and Loss Coefficient in Micro-Turbine Nozzle Vane (from ref. [41]).

A comprehensive analysis of the flow trough micro-turbomachinery is presented in [41] and the diagram in fig. 2.23 gives an impressive idea of both the Reynolds number range and of the exit flow angle downstream of a radial flow vane cascade.

One of the widest fields of investigation in the MGT area concerns the plant thermodynamics, also for combined heat and power production, and the component fluid-dynamics and design [42-70]. These studies are addressed to both the analysis and the design of either the whole plant or of a single stationary or rotating component. The latter aspects presents numerous examples [52, 60, 62, 69, 70]. In particular, ref. [52] presents a comprehensive study of a centrifugal compressor for a 100 kW microturbine, including the experimental investigation, the numerical simulation of the stator-rotor interaction and the diffuser optimisation as well. A sketch of the whole system analysed is provided in fig. 2.23.

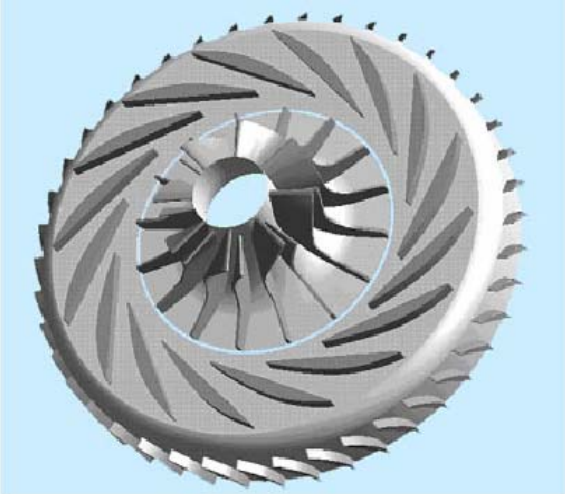

Figure 2.23: Rotor-Stator Assembly of a Centrifugal Compressor for a 100 kW Microturbine (from ref. [52]).

The authors of ref. [60] have carried out the design and prototyping of a fully radial micro gas turbine, whose general concepts and CAD schematics is displayed in fig. 2.24. In papers [69, 70] the CFD inverse design is applied to the definition of both the compressor and the turbine of MGT system fig. 2.25. The study is a completed by the finite-element based stress analysis of the rotors.

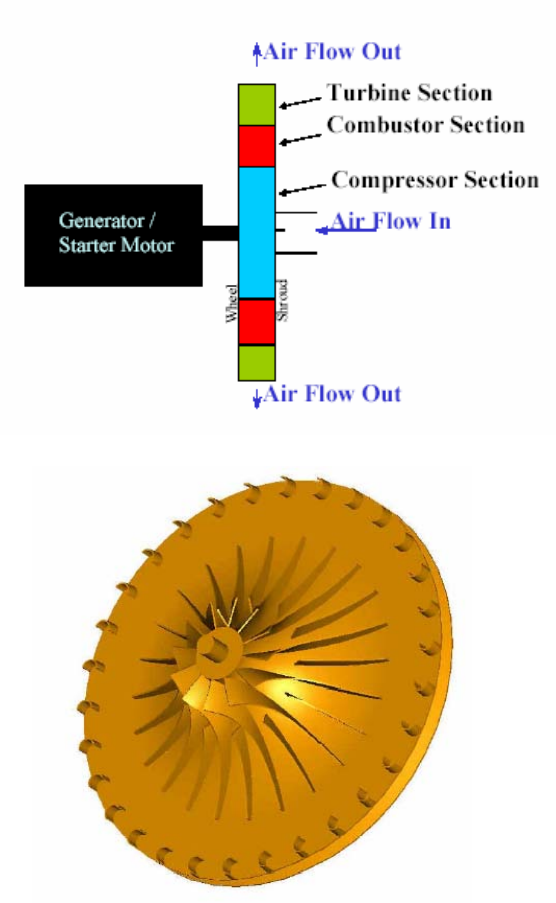

Figure 2.24: A Fully Centrifugal Microturbine (from ref. [60]).

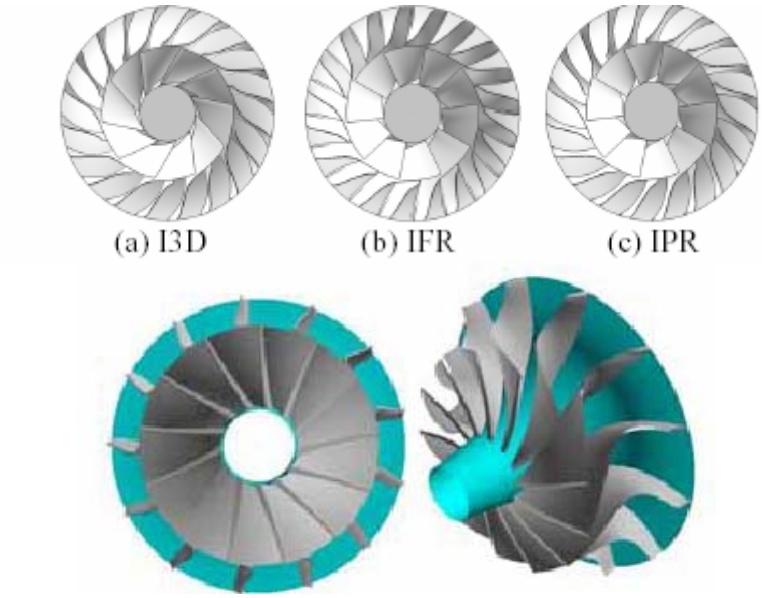

Figure 2.25: Progress in the Inverse Design of the Centrifugal Impeller and Final Geometry of the Expander of a Microturbine (from ref. [69, 70]).

The importance of the internal heat recuperator has been already stated and the search of both compact and efficient devices is currently carried out by many authors. Besides the previously listed examples, a rotating disk regenerator has been conceived and tested in ref. [62]. Although the basic idea is not innovative at all, its application to the micro-gas turbine promises advantages in terms of compactness of the system assembly and of optimisation of both the gas flows from the turbine and of the hot air flow to the burner (fig. 2.26).

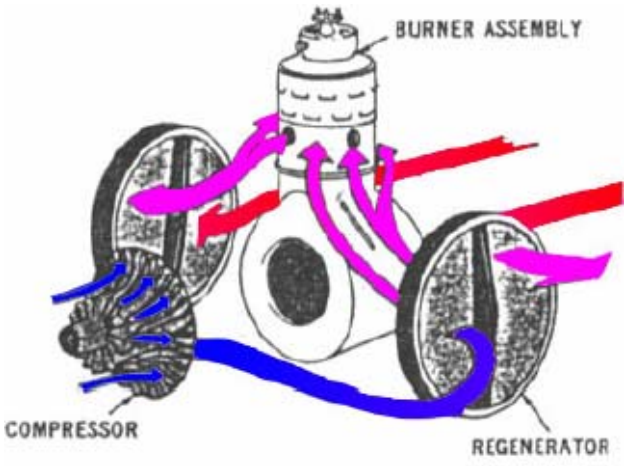

Figure 2.26: The Twin Rotating Disk Regenerator Concept (from ref. [62]).

The plant design and analysis founds on the choice of proper cycle options. Despite the multiplicity of possible configurations which have been recalled in fig. 2.1 [44], the trend of both researchers and manufacturers is undoubtedly converging to the open-cycle arrangement with the internal recuperator. Since many applications of the micro-gas turbine are oriented to the combined heat and power generation, it is currently accepted the plant flexibility can be enhanced by a variably recuperated cycle. This option can be activated through the partial by-pass of the recuperator, as a tool for obtaining a variable heat output [50, 59].

The estimation of the power plant performance as a function of the recuperator by-pass level will be widely discussed in the next sections, but it must be reminded hereby that also this proposal consists of the practical application of a really old-dated concept (i.e., the van Nest's patent in fig. 2.27). The same figure displays the (T-s) diagram of the thermal cycle with a variable level of the internal heat recovery.

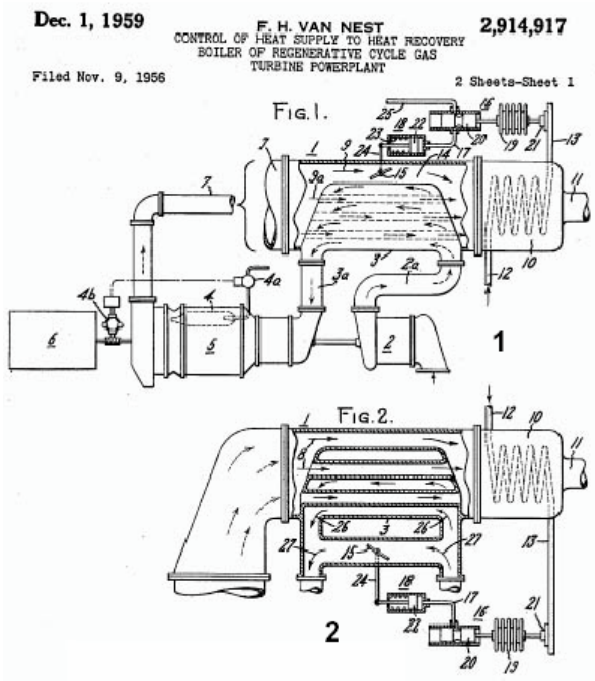

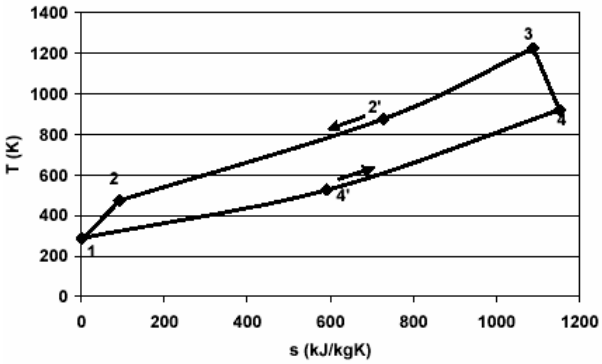

Figure 2.27: Schematics of the Van Nest's Patent and Diagram of the Variably Recuperated Cycle (from ref. [59]).

A further option which is widely proposed is the humid air cycle as a typical option for both enhancing the plant performance and compensating the changes in inlet air temperature, [57, 58, 66]. In particular, the authors of papers [57, 58] propose a basic HAT scheme and an enhanced one which includes an after-cooler for optimising the water-air mixing in the saturator, so reducing the energy losses (fig. 2.28). The authors in [66] concentrate the attention on the control of both the HAT line and the WAC line at the compressor inlet (fig. 2.29). Both systems are also conceived for cogenerating application.

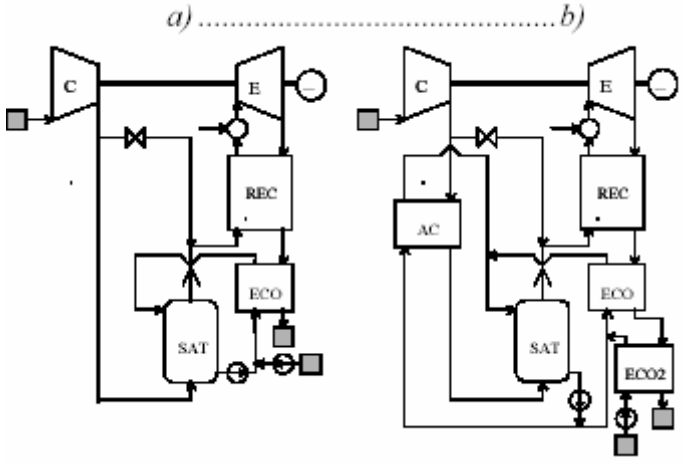

Figure 2.28: Schematics of Humid Air MGT (from ref. [57,58]).

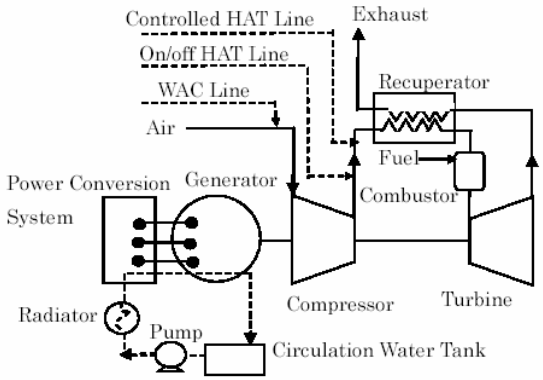

Figure 2.29: Layout of a HAT Based MGT (from ref. [66]).

The employment of MGT based plants for combined heat and power production is one of the most attractive features of these low-range energy conversion systems and many authors have been dealing in recent papers with several aspects related with the cogeneration with micro-gas turbines [43, 46, 49, 50, 53, 55, 56, 59, 65, 67, 68]. Besides the developing studies, many installations are already existing and an example form ref. [55] is displayed in fig. 2.30, which refers to a cogeneration system based on two 30kW Capstone microturbines. The example in fig. 2.31 displays a plant layout with a chiller/heater absorption system [46].

Figure 2.30: The Cogeneration System with two 30 kW Capstone MGTs (from ref. [55]).

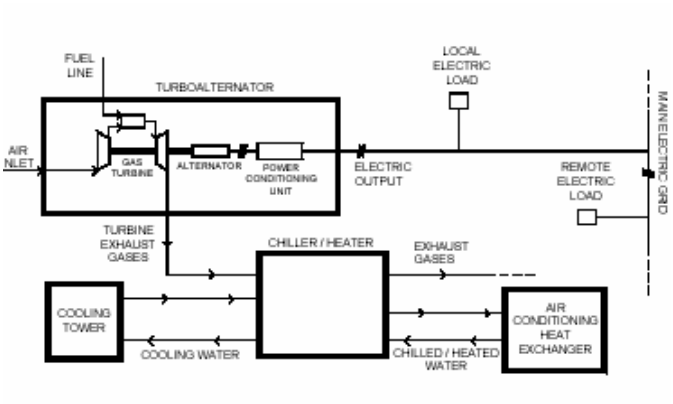

Figure 2.31: Layout of MGT Based Cogenerating Plant with Chiller/Heater Absorption Group (from ref. [46]).

The combined generation of electric power and of heat or chill, say the "trigeneration", is a further possibility for enhancing the attractiveness of the micro-gas turbines. Examples of exhaustive analyses of MGT based trigeneration systems can be found in papers [49, 53] which deal with this topic under many points of view: the authors start from a thermodynamic assessment and they proceed with the influence of the MGT characteristics on the plant performance and they finally achieve optimization of the combined plant, by also accounting for thermo-economic considerations. Figure 2.32 presents a layout of a plant for trigeneration.

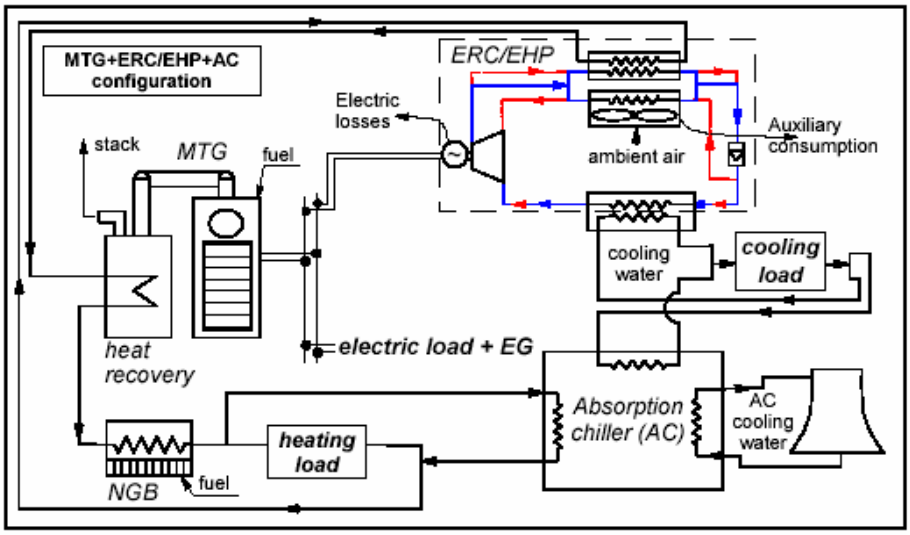

Figure 2.32: Layout of a MGT Based Plant for Trigeneration (from ref. [49, 53]).

A final topic of interest when analysing the MGT power plants is the study of the transient behaviour and examples in this sense can be found in recent papers [71-75]. The general purpose is both evaluating the plant response characteristics and identifying the most critical components that induce the longest delays. Such studies are also addressed to the determination of optimal fuel control laws, in order to prevent the occurrence of peaks in either shaft speed or firing temperatures. Papers [71, 72] present the study of MGT based plants also of the externally fired and of the closed cycle type. A typical shaft speed response is displayed in fig. 2.33, which refers to the early transient phase whose duration is extremely brief. This phase is followed by a second, much longer one with a slow achievement of the new steady regime, whose duration is typically of the order of magnitude of 10^2 s. The development of the slower phase is governed by the response characteristics of the heat exchangers and this aspect will be widely discussed in the final section of this paper.

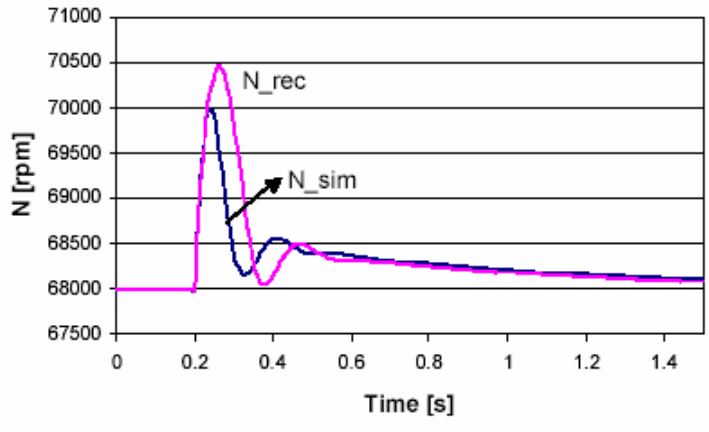

Figure 2.33: Transient Response of the MGT Shaft Speed (from ref. [71]).

3. CYCLE ANALYSIS OF THE MICRO-GAS TURBINE

The typical thermal cycle of a micro-gas turbine is characterized by rather unusual values of the base parameters, compared with those of higher range gas turbines (fig. 3.1), say:

- The pressure ratio results from the performance of a single centrifugal compressor derived from the either the turbocharging or the aircraft-engine technology so yielding values between 3 and 5.
- The turbine inlet temperature is chosen in accordance with the necessity of manufacturing the *MGT* without an excess in material costs and also of reducing the cooling air requirements. Therefore a T.I.T. in the range (1100 – 1250 K) is to be expected. The comparison of the *MGT* thermal cycle with the one of an up-to-date, heavy-duty gas turbine highlights that the micro-gas turbine operates with a reduced specific power and a poor efficiency level results from the cycle characteristics.
- On the other hand, the high temperatures at the end of the expansion would lead to an unlikely matching of the micro-gas turbine with heat recovery devices, which are usually addressed to a medium-low temperature heat utilization.
- The last consideration, together with the low efficiency levels for simple-cycle operation, suggests the necessity of adopting a recuperated cycle in order to exploit the large temperature difference between compressed air and exhaust gases within an internal recovery process. This results in both more competitive levels of the *MGT* efficiency and more reasonable temperatures at the inlet of a heat recovery boiler.

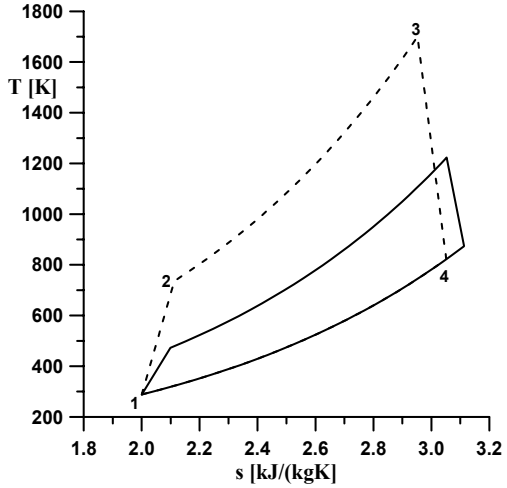

Figure 3.1: Thermal Cycle of a *MGT* Compared with the one of a Heavy-Duty Gas Turbine (dashed lines).

In order to provide a comprehensive sketch of the typical *MGT* potentials for cogeneration applications, the table 3.1 summarizes the energetic performance of a micro-gas turbines with a rated mechanical output of 110 kW (nearly 100 kW of electrical power).

Table 3.1: Typical Basic Data and Energetic Performance of a Micro-Gas Turbine

MGT DATA	
Mech. Arrangement	Single Shaft
Pressure Ratio	3.9
Compressor Politropic Efficiency	0.80
Turbine Politropic Efficiency	0.83
Recuperator Efficiency	0.877
Compressor Exit Temp.	468 K
Combustor Inlet Temp. (Fully regenerative cycle)	905 K
Turbine Inlet Temp.	1223 K
Turbine Exit Temp.	951 K
Recuperator Exit temp. (Fully regenerative cycle)	530 K
Rated Mechanical Output	110 kW
Nominal Speed	64000 rpm
Compressor, Turbine	Radial Flow
ENERGETIC PERFORMANCE	
Rated Mechanical Output	110 kW
Thermal Efficiency	0.340
Stack Temperature	403 K
Steam / Air ratio	0.0573
Thermal Output	108 kW
Fuel Energy Utilization Factor	0.670
Fuel Energy Saving Ratio	23.25 %

The value attained for the thermal efficiency results from a fully recuperated cycle and a key role is therefore played by the efficiency of the internal heat exchanger. The most up-to-dated technology leads nowadays to recuperator efficiencies close to 0.90 which lead to combustion inlet temperatures similar to that indicated in table 3.1.

The above results are derived from a simply thermodynamic simulation for natural gas fuelling and they confirm that a limited potential in terms of energetic performance is exhibited by the *MGT* also at base rating conditions. The saturated steam production refers to a saturation pressure of 1 bar, thus to a low temperature heat recovery case. Nevertheless, the energy saving ratio appears to be at the lowest acceptable margins for an efficient cogenerating operation.

Therefore, the attractiveness of the *MGT* employment must be enhanced by some solutions for both extending its operating range and adapting the output to a wide variety of electrical and thermal requirements. The first issue typically implies a variable-speed operation and it must be examined by advanced methods for *MGT* analysis, as discussed in the following section. The second one is partly dependent on the variable frequency electrical generation but it also involves the possibility of increasing the thermal output under particular conditions for the thermal output demand.

The plant layout in figure 3.2 [50] responds to the need of different thermal to mechanical load ratios through the solution of a partial by-pass of the internal recuperator. The exhaust fraction which by-passes the heat exchanger and is directly addressed to the heat recovery boiler is governed by the non-dimensional ratio:

$$X_b = 1 - \frac{\dot{m}_{g,R}}{\dot{m}_g} \tag{3.1}$$

where $X_b = 0$ leads to a fully recuperated cycle, while $X_b > 0$ increases the amount of thermal output for district or industrial heating.

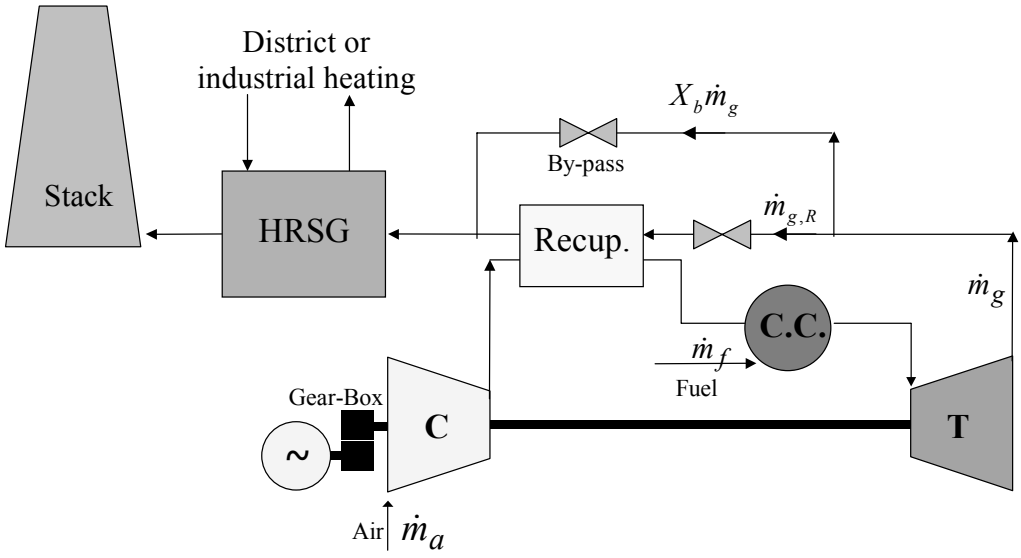

Figure 3.2: Layout of a MGT Based Cogenerating Plant with the Recuperator By-Pass.

In the following the situation with $X_b = 0$ will be referred to as "fully recuperated cycle" and it will involve the maximum temperature at combustor inlet (fig. 3.3). Conversely, the minimum in HRSG inlet

temperature is obtained and the energetic performance are those already presented in table 3.3. Increasing the X_b by-pass ratio produces a progressive decrease in the combustor inlet temperature and therefore in the cycle efficiency, but the rise in exhaust temperature in the HRSG allows larger thermal outputs, when needed. Of course, keeping the same T.I.T. level involves increased fuel flow rates, $\dot{m}_f$. Consequently, the activation of the recuperator by-pass option implies changes in the combustor operation due to the variations in both air inlet temperature and fuel/air ratios. The improvements in plant flexibility suggested by the thermodynamic analysis must therefore comply with the preservation of an efficient off-design behaviour of the combustor.

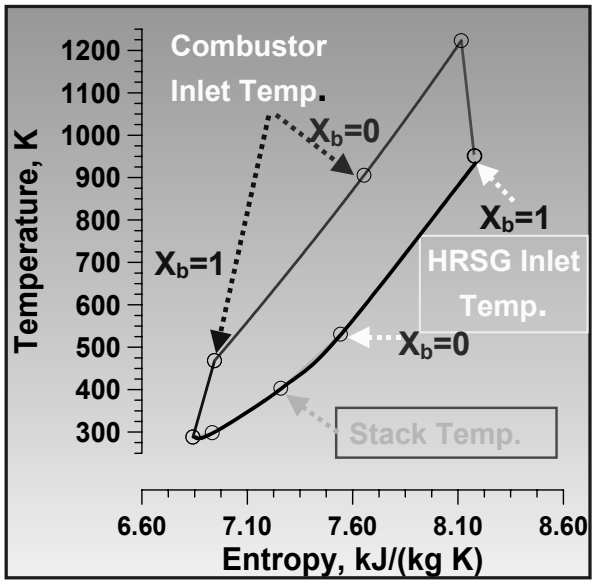

Figure 3.3: The Variably Recuperated Cycle.

Figure 3.4 summarizes the expected trend of the operating and performance parameters as functions of the recuperator by-pass ratio. The expected changes for the temperatures at combustor and boiler inlet, respectively induce diminution for the cycle efficiency and some evident benefits in terms of recoverable heat. The by-pass option must however be intended as a provisional tool for meeting an increased heat demand: really, the increased energy utilization factor is obtained at the expense of the cycle thermodynamics and this results in a progressive decrease in the energy saving ratio.

The diagram in figure 3.4(d) confirms that activating the recuperator by-pass is substantially addressed to a rise in steam production, but this kind of increase in thermal output conflicts with the preservation of a favourable mechanical / thermal output ratio so inducing worse conditions for the usual energy saving requirements. More encouraging considerations can be drawn if looking at the *MGT* plant in terms of investment costs and simplicity of installation: under these points of view, the adoption of the "variably recuperated cycle" allows avoiding auxiliary boilers at the same time ensuring a satisfactory flexibility. The latter can be further enhanced by the adoption of the variable-speed operation so leading to an attractive solution for the distributed, stand-alone, energy production.

It should be reminded that the results in figure 3.4 display the expected performance in the whole X_b range, starting from the "fully-recuperated cycle" up to the "full cogeneration" condition. The upper limit involves an excess in the *HSRG* inlet temperature which would be probably unacceptable, unless increased material costs are allowed. The practical, more realistic, application of the by-pass option must lie therefore in a reduced range of the X_b values.

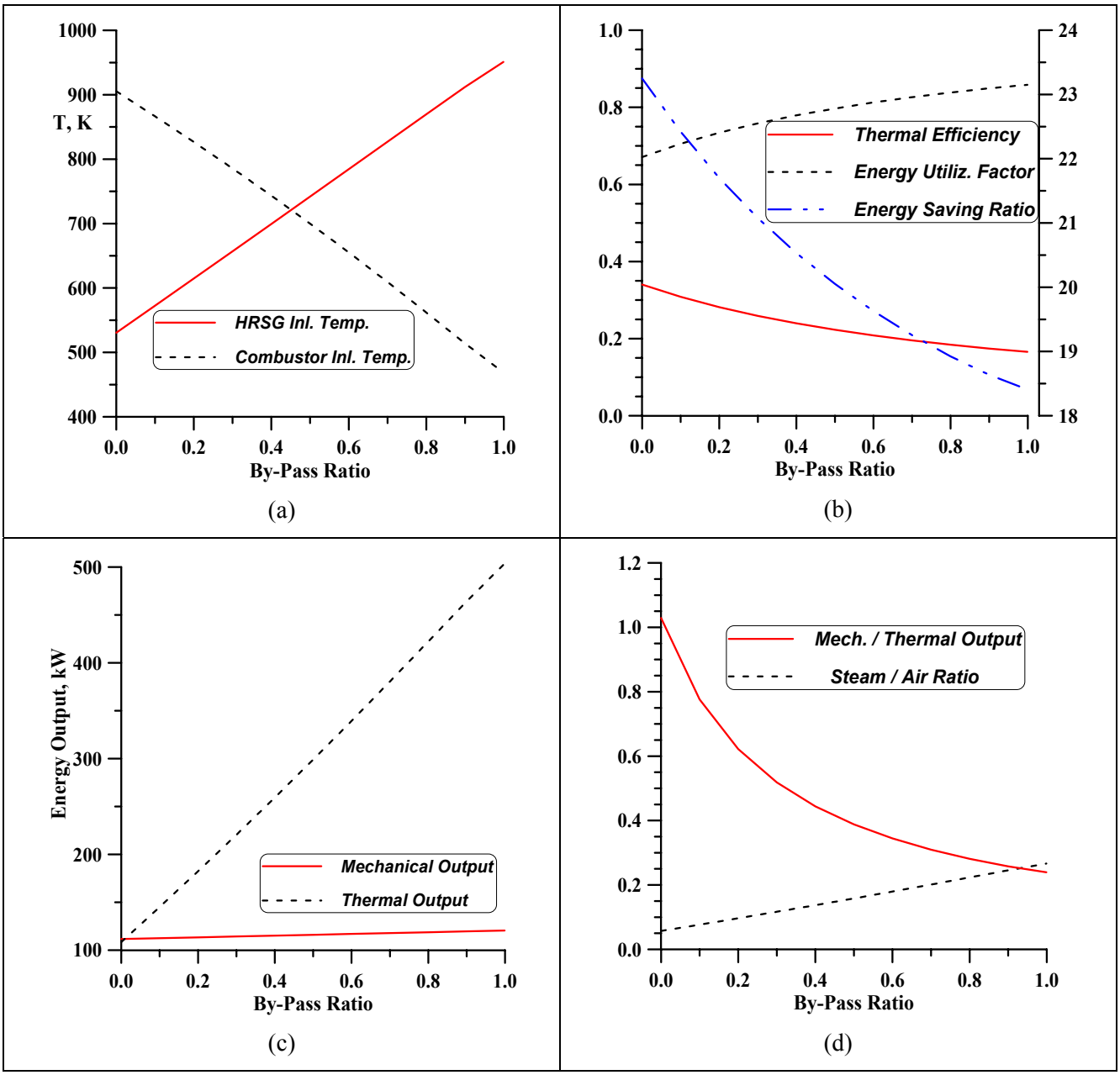

Figure 3.4: Trend of Operating and Performance Parameters with the Recuperator By-Pass Ratio.

An additional feature of interest for a wide use of *MGT* based plants is the employment of different fuels, like those originating from the gasification of either bio-masses or solid wastes. Table 3.2 compares the composition and the thermo-chemical properties of a typical natural gas with some examples of alternative fuels. In particular the *BIOM(O)* and *BIOM(a)* ones are derived from two distinct gasification processes, say oxygen or air based respectively, while the *SW* acronym designates a gaseous fuel from solid waste pyrolysis [30, 32].

Table 3.2: Natural Gas and Gaseous Fuels from Bio-Mass and Solid Waste Gasification Composition and Properties

Fuel Composition (%, molar)	Nat. Gas (*NG*)	*BIOM(O)*	*BIOM(a)*	*SW*
CH4	**92.00**	**18.00**	**9.00**	**7.00**
C2H6	3.70	2.00	- -	7.00
C3H8	1.00	2.00	- -	7.00
C4H10	0.25	2.00	- -	- -
N2	2.90	8.00	56.00	- -
H2	**- -**	**25.00**	**9.00**	**18.00**
CO	- -	33.00	12.00	61.00
CO2	0.15	10.00	20.00	- -
H2O	- -	- -	- -	- -
Mol. Mass, g/mol	17.34	21.92	28.51	23.76
LHV, kJ/kg	47182	19198	2798	21697
h_{0f}, kJ/kg	-4266.9	-3720.1	-1649.5	-2923.9
f_{st}	0.0620	0.1680	1.257	0.1530
T_{of}, *K*	2220	2231	1571	2300

The *BIOM(O)* and *SW* fuels are of the medium LHV class and both present an adiabatic flame temperature somewhat higher than for the natural gas, due to the significant hydrogen contents and the poor percentage of inert species. On the contrary, the *BIOM(a)* fuel is a typical low LHV gas obtainable from a less expensive gasification process and with considerable N2 and CO2 contents. This case will be worthy of special attention in the next section because its use involves relevant changes in the mass flow rate through the turbine and the consequent alterations in the matching conditions with the compressor.

The last examples in this section are presented to the sake of a complete overview of the *MGT* performance and refer to the comparison of the different fuels in table 3.2, in terms of expected energetic behaviour with the recuperator by-pass ratio.

The results in figures 3.5 and 3.6 are derived from a previous author's paper [50] and are obtained by imposing the same values for the cycle parameters, i.e. pressure ratio and T.I.T., with the same air flow rate at base rating, according to the values given in table 3.1. With this assumption, both mechanical and thermal output increase with the gas flow rate through the turbine and in this sense the highest values are attained with the *BIOM(a)* gas which requires the largest fuel/air ratio. A general trend of increasing outputs with the stoichiometric ratio is clearly observed in figures 3.5(a) and 2.5(b).

The reason for the different pattern of the thermal efficiency (fig. 3.5c) is that the cycle specific work (for unit air mass) decreases for the low LHV fuels which require a larger amount of compression work; in addition, an increasing fraction of the combustion heat is absorbed by the mass of fuel itself. This implies that the heat addition must be larger when low LHV fuels are introduced, with a consequent drawback for the cycle efficiency. Finally, the energy saving ratio seems to take advantage of the employment of low LHV fuels, since this parameter is also sensitive to the thermal output whose effect overcomes that of the reduced thermal efficiency. The results in figure 3.5(d) only consider the energetic performance of the micro-gas turbine and the additional costs for the fuel gasification process are neglected: this explains the higher levels associated with the *BIOM(a)* gas. In any case, the interesting energetic results related to the bio-mass or solid waste derived fuels can be intended as a further

encouragement to the employment of alternative fuels, besides the express indication contained in the laws of many European countries relating the use of alternate energy sources.

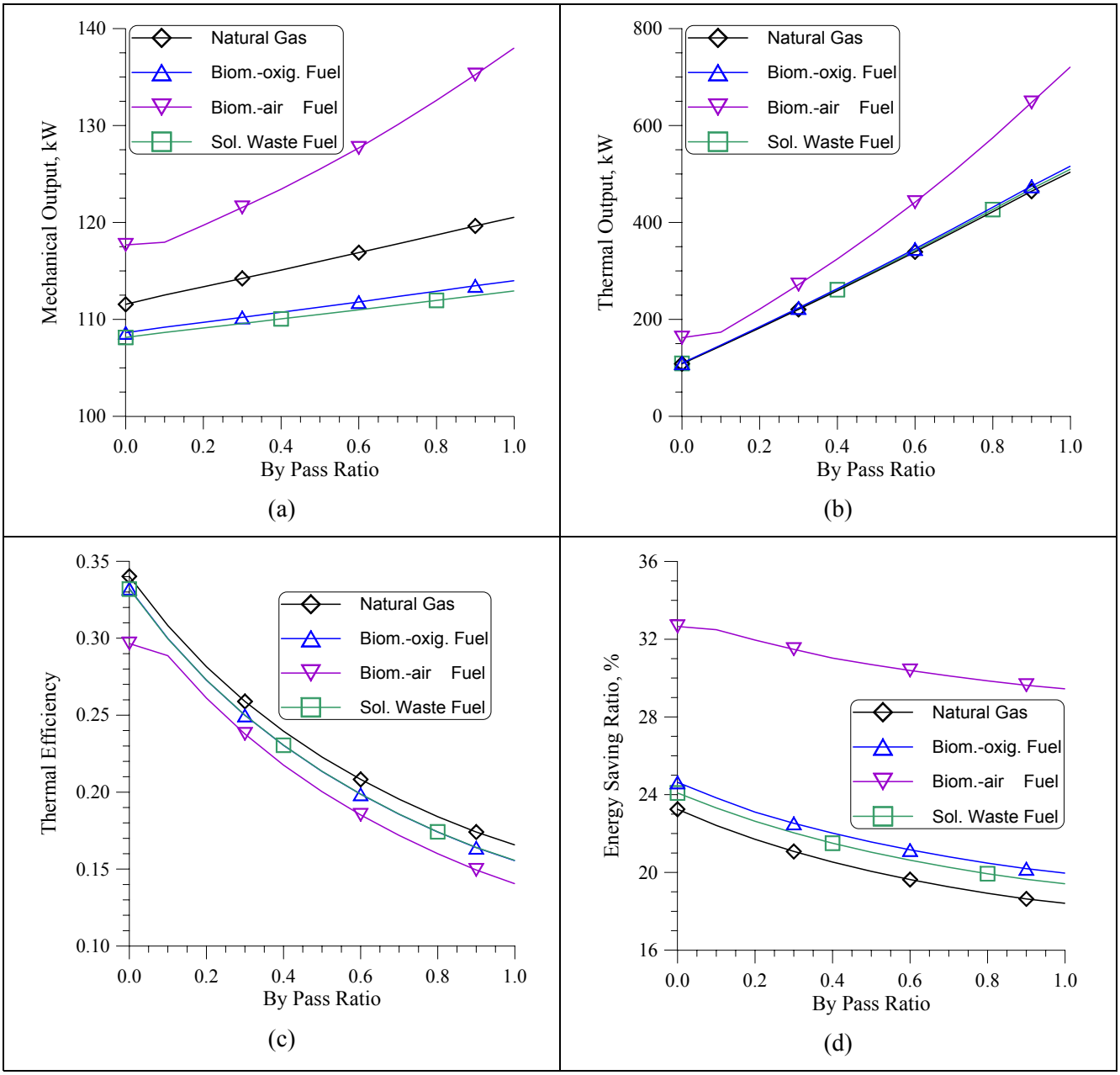

Figure 3.5: Performance Data of the *MGT* Supplied with Different Fuels vs. the By-Pass Ratio.

A concluding remark of this section refers to the expected emission of pollutants and greenhouse effect species. The figure 3.6 compares the predicted trends of the thermal NO concentrations and of the CO2 emission index with the X_b parameter for the several fuels already considered in figure 3.5. The carbon dioxide index obviously increases with the by-pass ratio because of the rise in specific fuel consumption, but the values are generally unacceptable specially when adopting poor LHV fuels. The index refers only to the mechanical energy production and more acceptable values can be obtained for a combined heat and electricity generation, as an additional reason for operating the *MGT* within a cogenerating plant.

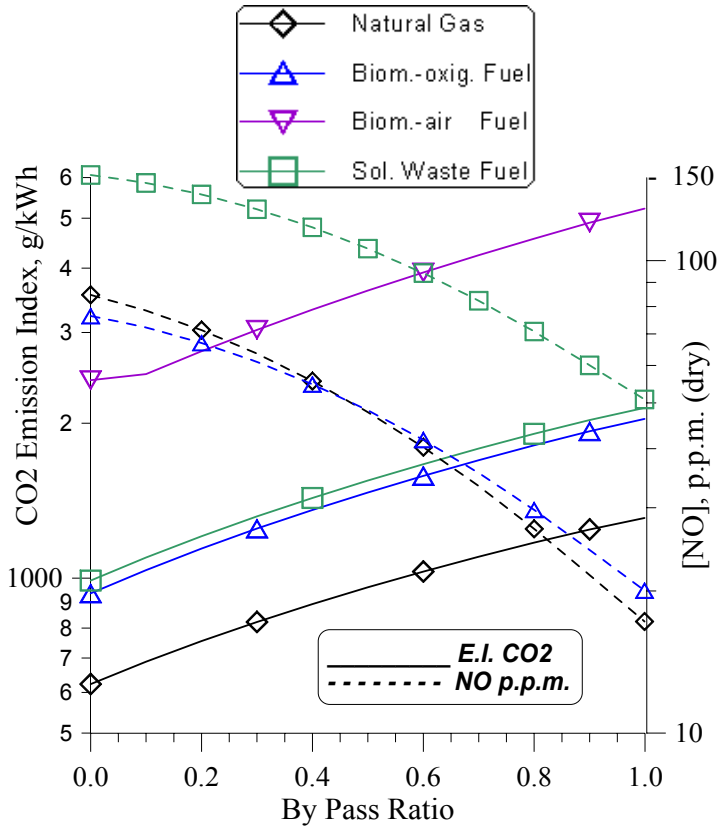

Figure 3.6: Expected Emission Levels of the MGT with Different Fuels.

Regarding to the nitric oxide emission, the values in fig. 3.6 were obtained with a thermo-kinetic model [50, 82, 83] under the hypothesis of a typical diffusive combustion with a unit primary equivalence ratio. The decreasing trend with the recuperator by-pass ratio is explained by the diminution in combustor inlet temperature.

The highest levels, as expected, are reached by the *SW* fuel while those from the BIOM(a) employment are fairly negligible, due to the very low adiabatic flame temperature. The reliability of this results must be however checked by a more detailed combustion analysis. In particular, the low LHV fuels would probably present problems in terms of flammability limits and self-ignition: therefore the adoption of a lean-premixed line could be non-favourable to the combustion progress. More realistic solutions are those with a mixture of natural gas with bio-mass derived gases, so that the results in the previous figures are to be intended as the ones obtainable from the employment of pure alternative fuels.

4. METHODS FOR PERFORMANCE EVALUATION

As described in the previous section, the main interest in micro-gas turbine based energy conversion systems consists of the possibility of ensuring a satisfactory operation in a wide range of electrical and thermal loads. The previously mentioned tools for extending the *MGT* operating field, i.e., with both variable speed and partly recuperated cycles, induce off-design condition in each rotating component and in the matching of the several devices. Therefore a simple cycle analysis, like that discussed before, may provide preliminary indications to be more accurately investigated by means of an off-design simulation of the *MGT* based power plant.

4.1 The *MGT* Operating Region

The method outlined in the following has been proposed since many years by the authors and applies to a wide variety of gas turbine based systems, both of the simple and of the combined cycle, and it is generally addressed to examine each innovation which is introduced either to enhance the plant efficiency or to enlarge its operating range. Furthermore, the analysis aims at a deeper investigation of the effects of the introduction of low LHV fuels which involve a considerable mass addition to the expanding gases.

The methodology founds on the employment of the compressor and turbine maps. Fig. 4.1 displays the radial compressor and turbine characteristics of the 110 kW *MGT* described before and the matching model has the purpose of finding the actual operating region of the gas turbine within the compressor area. With reference to symbols in figures 3.1 and 3.2, the sequence of calculation can be outlined as follows:

$$\beta_c,\ \eta_c = f(\dot{m}_a, N, T_1, p_1) \quad \text{Compressor Map Accessed} \quad (4.1)$$

$$T_2, p_2, h_2, \ldots = f(\beta_c, \eta_c, T_1, p_1) \quad \text{Compression Calculation} \quad (4.2)$$

$$T_{2R}, p_{2R}, h_{2R}, \ldots = f(T_2, p_2, X_b, \eta_{rec}, \varepsilon_{rec}) \quad \text{Recuperator Calculation} \quad (4.3)$$

$$T_3, p_3, h_3, \ldots = f(\dot{m}_a, \dot{m}_f, T_2, p_2, h_2, \eta_b, \varepsilon_{cc}) \quad \text{Combustion Calculation} \quad (4.4)$$

$$\beta_t,\ \eta_t = f(\dot{m}_a + \dot{m}_f, N, T_3, p_3) \quad \text{Turbine Map Accessed} \quad (4.5)$$

$$T_4, p_4, h_4 = f(\beta_t, \eta_t, T_3, p_3) \quad \text{Expansion Calculation} \quad (4.6)$$

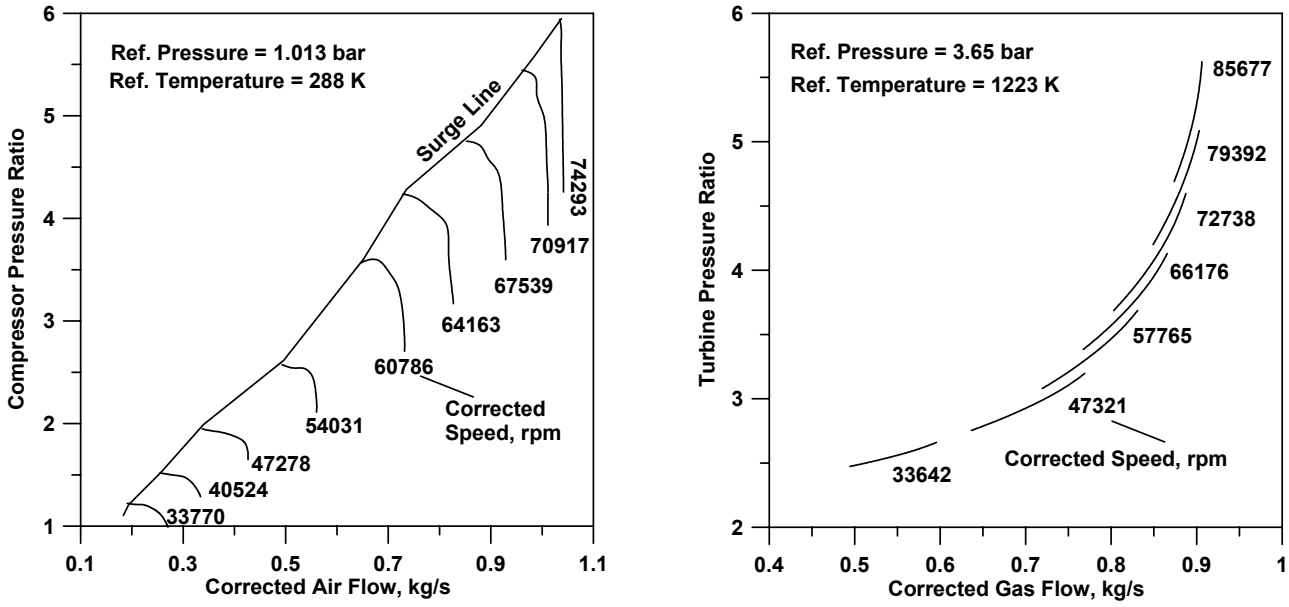

Figure 4.1: Typical Compressor and Turbine Characteristics for MGT Applications.

It is worth-noting that the results are also affected by the performance of the internal recuperating heat exchanger, in terms of recuperator efficiency, η_{rec}, and pressure loss coefficient, ε_{rec} . Both parameters depend on the actual gas flow rate through the hot and cold side channels and the correlation employed

[10, 13, 50] assumes as independent variable the gas to air ratio. The latter depend, of course, on both the fuel/air ratio, *f*, and on the by-pass ratio. The use of a low LHV fuel, like the *BIOM(a)* one, results in an increase of the gas/air ratio and consequently in less favourable values of recuperator efficiency and pressure drop (fig. 4.2).

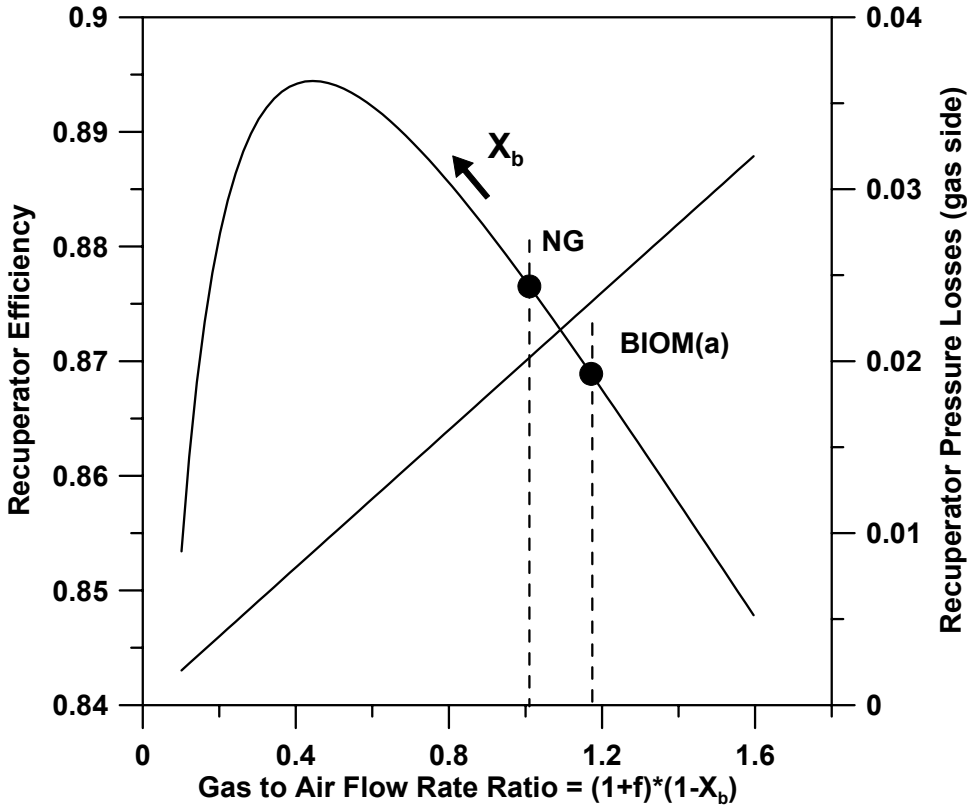

Figure 4.2: Correlation for Recuperator Efficiency and Pressure Losses.

The closure conditions is that the turbine discharge pressure, p_4, must equal the atmospheric pressure plus the pressure losses through the recuperator hot side, the heat recovery device and the stack:

$$p_4 \equiv p_{atm}\left(1+\varepsilon_{rec,H}+\varepsilon_{HRSG}+\varepsilon_{STK}\right) \tag{4.7}$$

On the other hand, the above computational (eqs. 4.1 – 4.6) sequence has demonstrated that the p_4 pressure is obtained as a function of three independent parameters:

$$p_4 \equiv f\left(\dot{m}_a, \dot{m}_f, N\right) \tag{4.8}$$

Therefore, solving equation (4.8) corresponds to setting up a two-degrees of freedom problem. In other words the air mass flow rate, $\dot{m}_a$, is the unknown variable of the matching problem and each solutions implies the $\dot{m}_a$ dependence on the pair of free variables $\left(\dot{m}_f, N\right)$:

$$p_4 \equiv p_{atm}\left(1+\varepsilon_{rec,H}+\varepsilon_{HRSG}+\varepsilon_{STK}\right) \Rightarrow \quad \dot{m}_a = \bar{f}\left(\dot{m}_a, N\right) \tag{4.9}$$

The solutions of the matching problem may be then represented in a two-dimensional space whose primitive variables are the fuel mass flow rate, $\dot{m}_f$, and the shaft rotational speed, *N*. The latter are really the main operating variables for adapting the *MGT* operation to the external load and the actual operating range is restricted within a domain whose boundaries are defined by the typical limitations of the rotating components, i.e., the compressor stall and choking and the turbine choking. The latter component undergoes, in particular, more severe variations in the corrected speed and mass flow rates, because of the changes which may occur in both the actual gas flow rate and in the turbine inlet pressure and temperature, p_3, T_3. This explains why the shape and the extension of the operating domain is specially sensitive of the kind of fuel adopted, since changes in the calorific value affect both the temperature rise through the combustor and the increase in the total mass flow rate.

As a first example of the results that can be obtained from the matching calculation, figures 4.3(a) and 4.3(b) display the micro-gas turbine operating domain in two different coordinate systems: the first one (fig. 4.3a) refers to the primitive pair of independent variables, in the non-dimensional form $\left(\dot{m}_f \middle/ \dot{m}_f^* , N \middle/ N^*\right)$, where the asterisk refers to the base-rating conditions, and this representation allows a clear identification of the restrictions imposed by the rotating components. In particular, the combined effect of the turbine and compressor choking conditions prevent a low-speed operation of the micro-gas turbine. Consequently, the second 2-D space (fig. 4.3b) in the physical plane (N, P) evidences the range of actual values of shaft speed and mechanical power which can be actually covered by the MGT. This diagram allows an easier investigation of the matching conditions of the MGT with external devices, like a constant or variable speed generator, as discussed in the following.

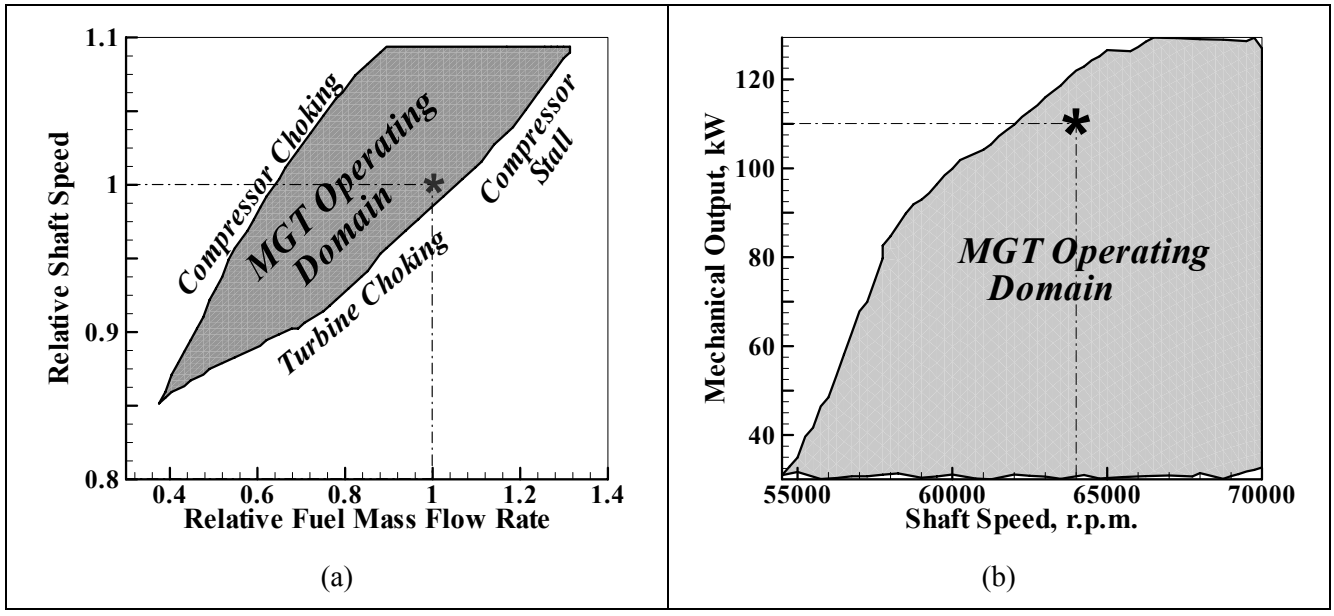

Figure 4.3: The MGT Operating Domains in two Different 2D Spaces.

As stated, the method is able to evaluate the actual portion of the compressor operating area that allows a proper matching with the other MGT components. This is highlighted by the direct display of the MGT domain in the plane of the compressor characteristic curves. The superimposition of the MGT domain (fig. 4.4a) to the compressor area (fig. 4.4b) puts into evidence the real effect of the limitations imposed by the matching conditions.

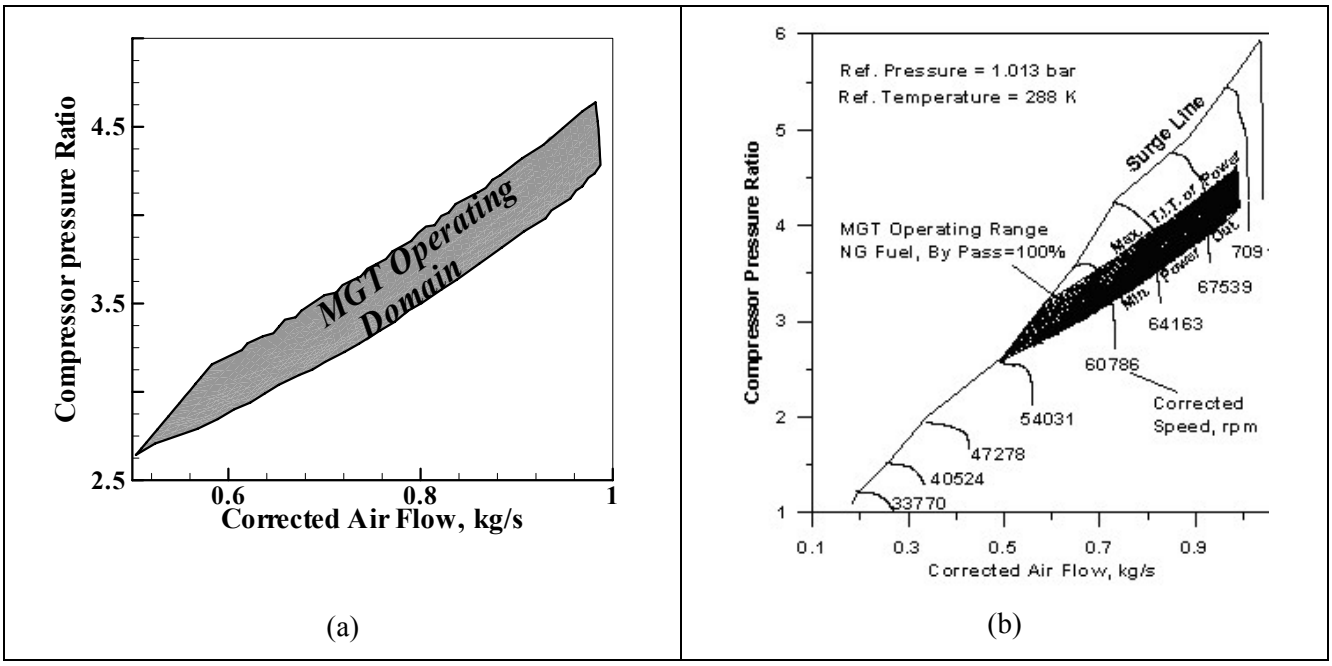

Figure 4.4: The MGT Domain in the Compressor Operating Plane.

The domain in fig. 4.3 and 4.4 being the locus of existing solutions of the matching problem, each point lying inside this region is identified by a different set of parameters which characterize the thermal cycle, the *MGT* operation, and the performance level as well. Examples of iso-level contours of these parameters are displayed in figure 4.4 and they give an impressive sketch of the changes which are expected in both operating conditions and performance for imposed variations to the base parameters, $\left(\dot{m}_f / \dot{m}_f^* , N/N^*\right)$. Of course, any constraint on the values displayed in fig. 4.5 (for instance, on the maximum turbine inlet temperature) produces a further restriction on the area of the *MGT* domain.

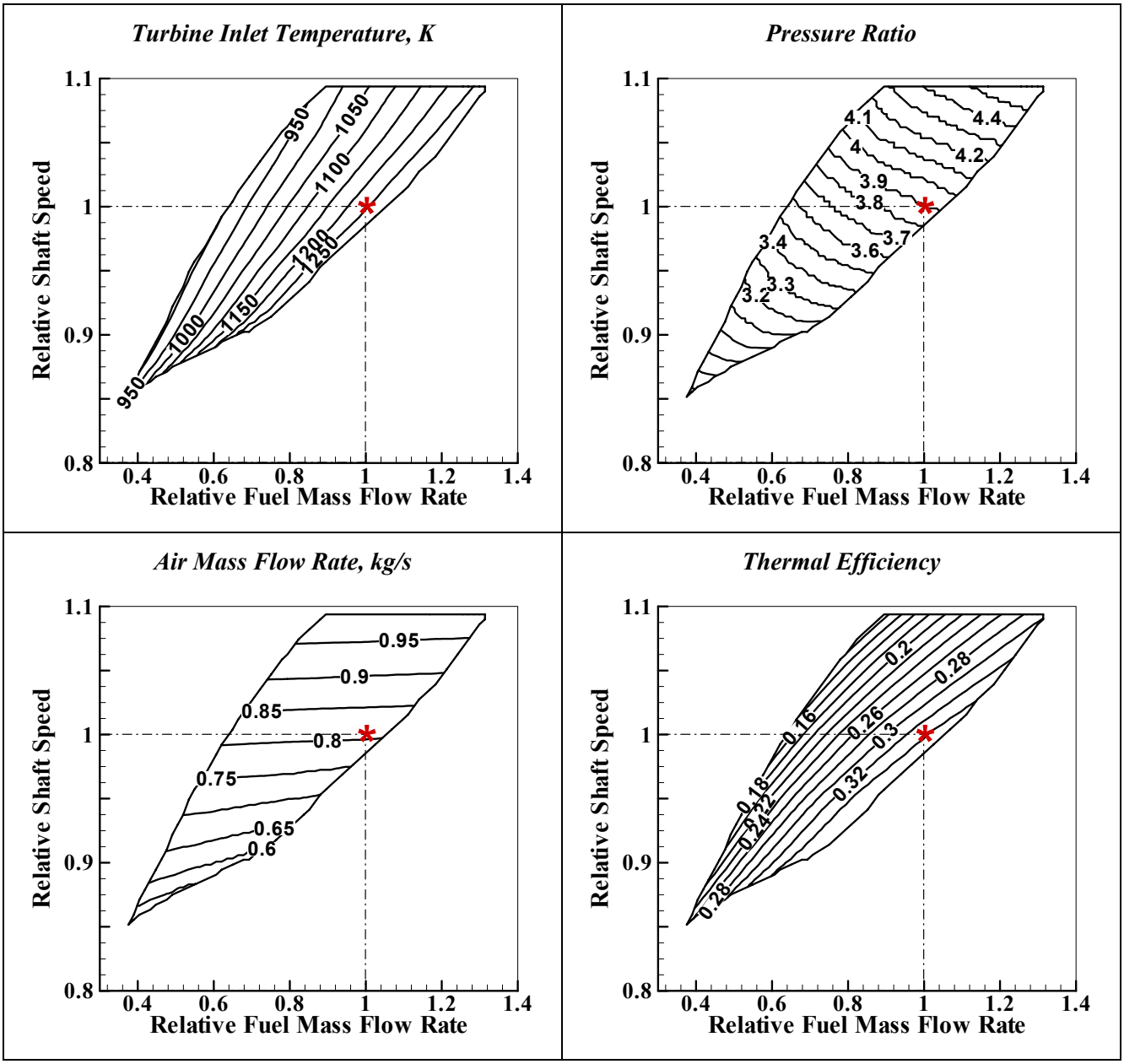

Figure 4.5: Contours of Cycle and Performance Parameters inside the MGT Domain.

As said above, the model may be also employed as to estimate the changes in the extent of the operating range when using different fuels, in particular those of the low-LHV type. The employment of this kind of fuels involves significant variations in the gas flow rate through the turbine. The occurrence of choking conditions may generally result in some reactions of the rotating system, say:

- The excess in gas flow rate may be compensated by a reduction in air mass flow rate, so leading the compressor closer to stall conditions;
- The compensation may also be achieved through a reduction in the turbine inlet temperature: the effect is somewhat amplified, since the turbine corrected speed increases, for a same actual rotating speed, and the choking limits are shifted forward. Simultaneously, an increased gas flow rate is accepted, because of the favourable influence of the temperature decrease on the corrected gas flow.

The first kind of reaction usually takes place in the gas generator system of twin-spool gas turbines. In the present case, the *MGT* system adapts its operation by the second way, so that the employment of the BIOM(a) fuel produces a slight enlargement of the operating region (figure 4.6), compared with the one for natural gas supply. The reason for this result arises from the location of the *MGT* domain in the compressor area (fig. 4.4). Really, the compressor operates far from the stall limits, except for low rotational speeds, and this makes it possible operating with reduced air mass flow rates when a larger fuel mass addition occurs. The major domain extent for the BIOM(a) fuelled *MGT* is a consequence of this situation and the main limits are only imposed by the turbine choking conditions.

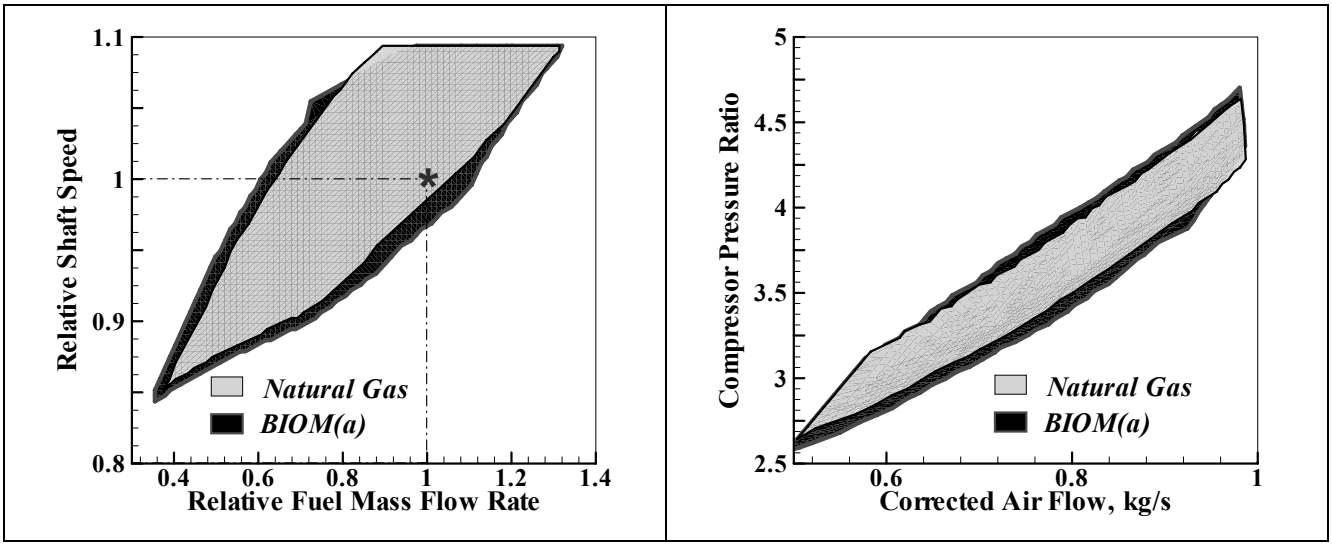

Figure 4.6: Comparison of MGT Domains for Natural Gas and BIOM(a) Fuelling.

The comparison of the *MGT* performance in the physical plane (*N*, *P*) under the two different fuelling conditions (fig. 4.7) confirms the above considerations: the main difference is evidently the decrease in turbine inlet temperature when the *BIOM(a)*, low LHV fuel, is supplied (fig. 4.7a). The same level of net mechanical output is reached because of the increased gas flow rate through the turbine, but a considerable difference exists between the "net mechanical power" and the "shaft power" because of the considerable amount of mechanical energy required for the fuel compression. This reason, together with the decreased mean temperature in the heat addition process, produces a relevant decrease in the thermal efficiency (fig. 4.7d). Minor variations, as expected, can be detected in the cycle pressure ratio (fig. 4.7b) and in the air mass flow rate (fig. 4.7c), even if the *BIOM(a)* operation allows a slight enlargement of the *MGT* domain in the range of the low compressor air flows.

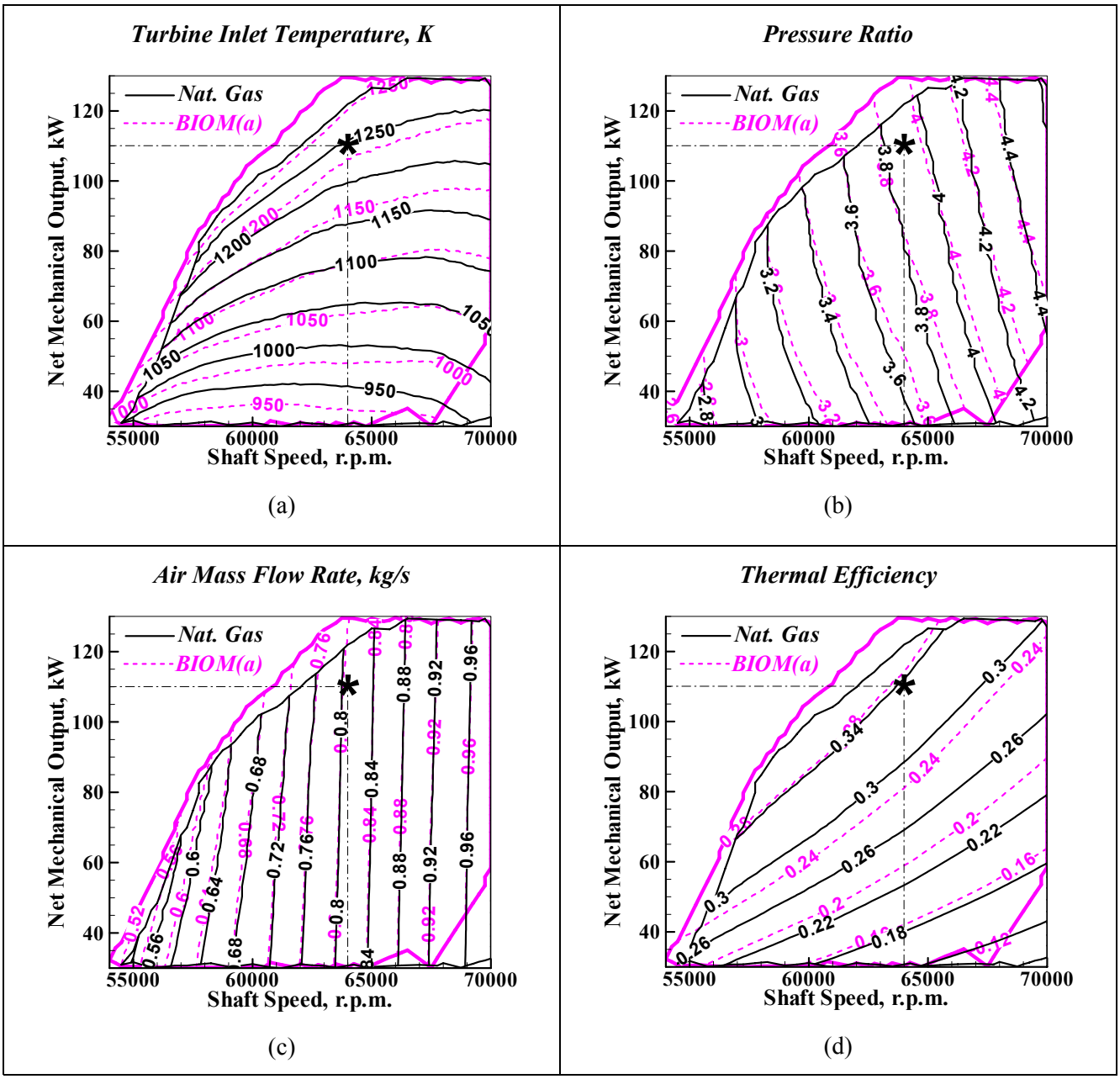

Figure 4.7: Cycle and Performance Parameters of the MGT with Different Fuels.

4.2 Operating with Fuel Mixtures

All the above examples refer to the employment of either natural gas or fuels directly obtained from the gasification of bio-masses or solid wastes. In order to enhance the flammability characteristics of the latter type of gaseous fuel it is usually more appropriate to make use of mixtures with natural gas. The following examples refer to a 50% mixture of the *BIOM(a)* fuel with natural gas and the results are for a variable-load, constant speed operation with the same methodology as the one discussed above.

Fig. 4.8 displays the trend of cycle parameters and the turbine operating parameters versus the net mechanical output for both the pure fuels and their mixture. As already stated the operation with the BIOM(a) fuel is characterized by a decreased turbine inlet temperature (fig. 4.8a) at the highest loads

which compensates the excess in turbine mass flow rate associated with the large fuel mass addition. The temperature decrease is also favourable for a higher turbine corrected speed (fig. 4.8c) which allows the larger corrected mass flows through the turbine (fig. 4.8d). The 50% mixture presents substantially intermediate trends but the results are generally closer to those of the natural gas fuelling, because the chosen mixture rate is enough for increasing the order of magnitude of the calorific value.

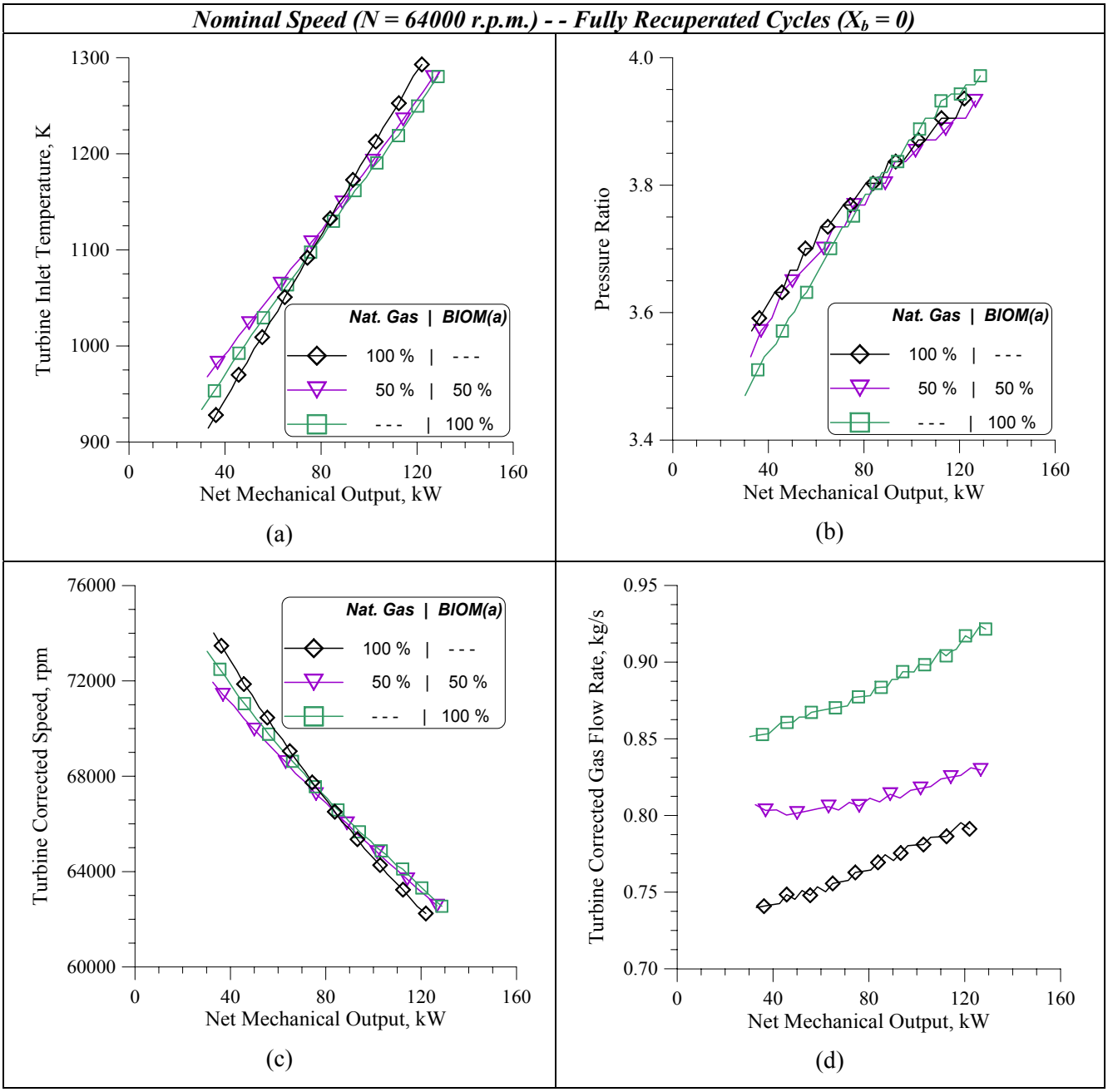

Figure 4.8: Cycle and Operating Parameters with Different Fuel Mixtures.

In terms of performance and emission levels (fig. 4.9), the mixture of natural gas and *BIOM(a)* presents much better results than the low-BTU, bio-mass gasified fuel, if looking at the thermal efficiency (fig. 4.9a) and at the CO_2 emission index. As expected, both levels are nearly the same as for the natural

gas fuelling. The specific carbon dioxide production (fig. 4.9b) is however unacceptable if referred to the production of mechanical energy only, so that the *MGT* operation within a cogenerating plant is in any case suggested.

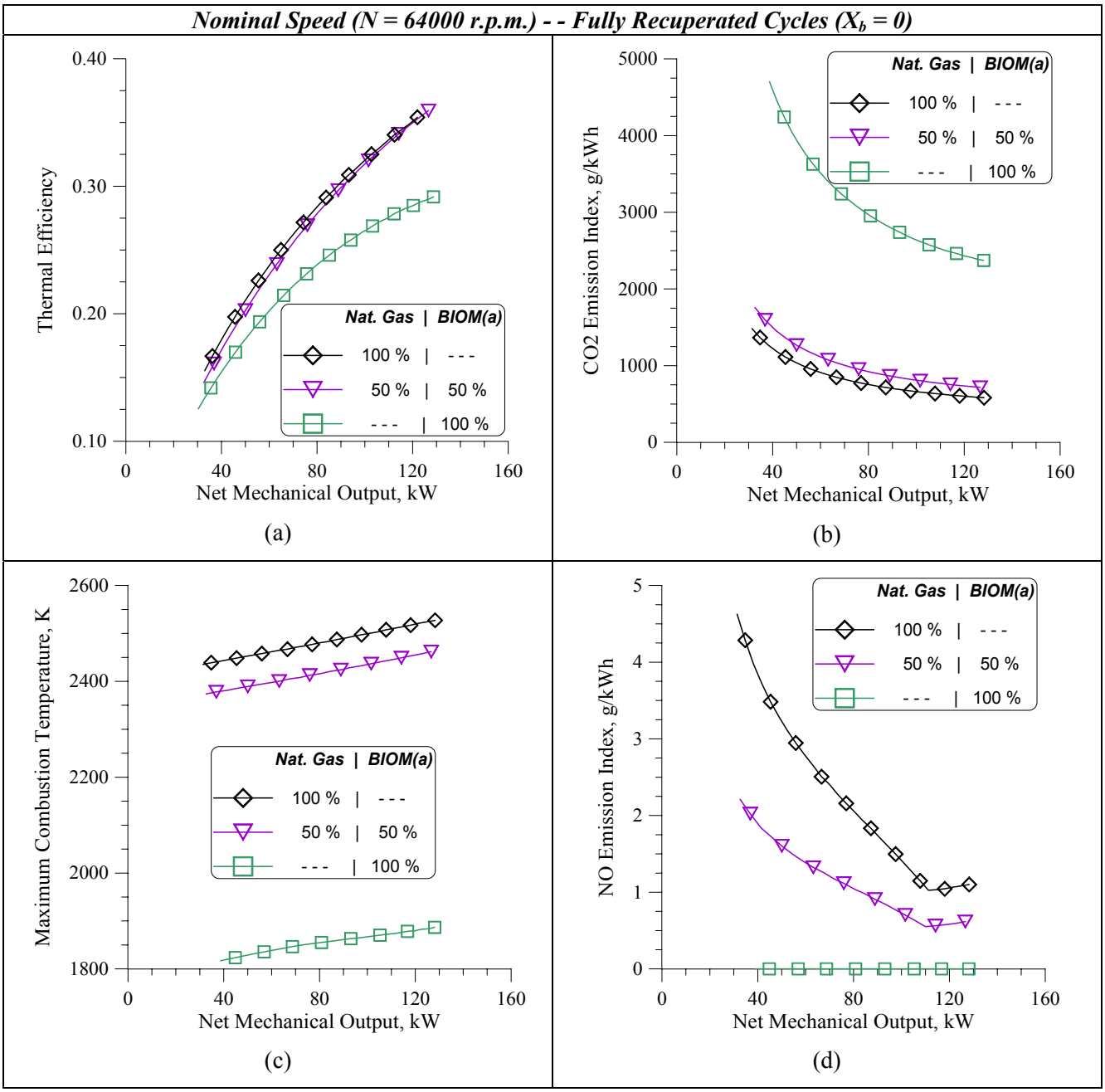

Figure 4.9: Efficiency and Emission Levels with Different Fuel Mixtures.

Regarding to the nitric thermal oxide, the increase in the calorific value of the fuel mixture also results in higher adiabatic flame temperatures, thus in higher maximum combustion temperatures (fig. 4.9c). Therefore, while in the *BIOM(a)* case the activation of the NO mechanism is practically negligible, both natural gas and the 50% mixture present significant reaction rates in the Zel'Dovich scheme, so that the employment of a lean primary fuel/air ratio is needed. The results in fig. 4.9(d), obtained with the thermo-

kinetic model, refer to a primary equivalence ratio of 0.521, but the combustion progress is sustained by a pilot flame. The amount of fuel to the pilot line is of 10% at base rating, but it linearly increases when the mechanical load decreases. This explains the trends of the NO emission indices that present a minimum for the 110 kW value. The 50% mixture seems a good compromise between the efficiency preservation and a significant reduction of nitric oxide emission.

4.3 Operation with Variable Electrical and Thermal Loads

Once examined the potential of the micro-gas turbine in terms of the extent of its operating field, also when fuelled with low BTU gases, the attention is now focused on the actual possibilities of fulfilling a wide variety of electrical or thermal requirements. It is to be recalled that good perspectives in this sense are offered by both the variable-speed operation (in the case of the *MGT* coupling with a variable-frequency alternator) and the recuperator by-pass option.

In this section we will refer to natural gas fuelling and in a first step the two options will be examined separately.

1) **Fully Recuperated Cycles, Variable-Speed Operation**. The already defined by-pass ratio, *Xb*, is zero and the operating area of the MGT has the shape presented in previous diagrams (figs. 4.3 – 4.5). The following figure 4.10 puts into evidence within the actual operating chart of the micro gas turbine some fundamental parameters, say:

   - The electrical load constant *K*, defined as:

$$\frac{P_{el}}{P*} = K\left(\frac{N}{N*}\right)^3 \tag{4.10}$$

     where a cubic response of the electrical power with the generator speed is hypothesized;

   - The relative fuel flow rate, $\dot{m}_f \Big/ \dot{m}_f^*$ (fig. 4.10a), or – more directly – the thermal efficiency (fig. 4.10b).

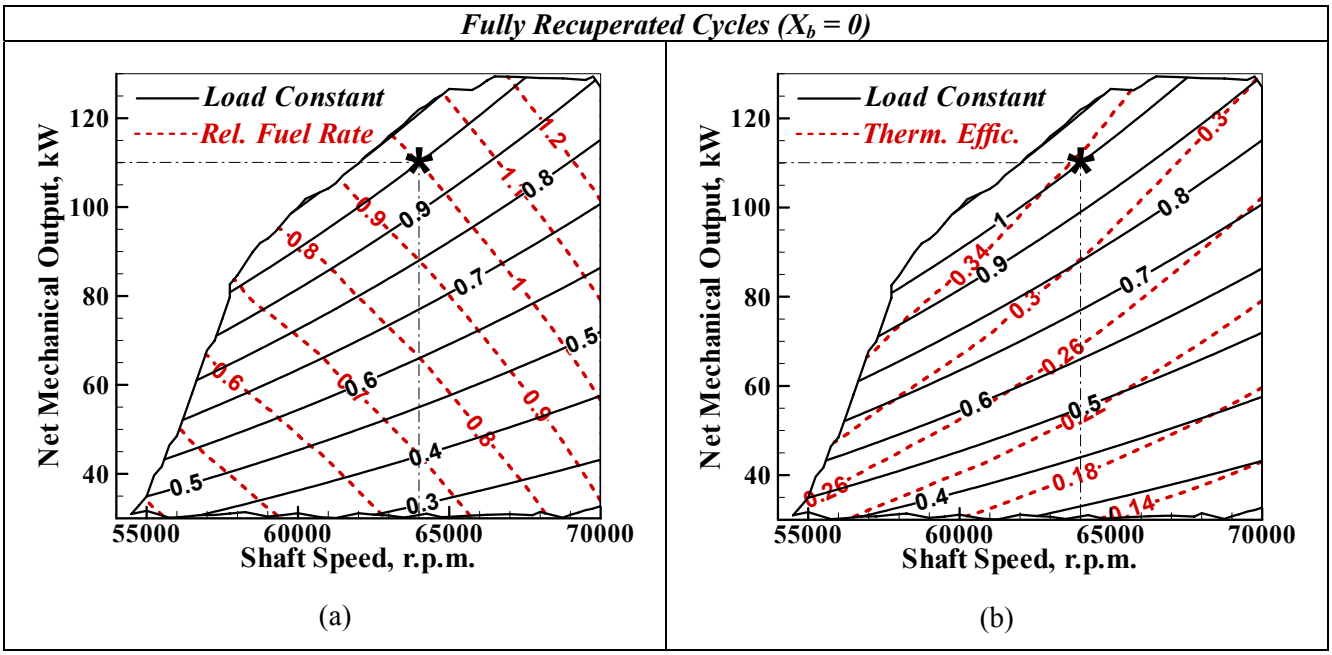

Figure 4.10: Characteristic Curves of the MGT within the Operating Region.

Both figures highlight that a constant-speed operation would involve the maximum fuel consumption, while following the iso-contour of the *K* load constant would ensure the preservation of the best efficiency levels. Of course, the actual regulation path for the *MGT* is governed by the real pattern of the electrical load within the operating plane, but both figures show that each load decrease followed by a shaft speed reduction would produce better results than a *MGT* response at the same nominal speed.

Regarding to the performance for combined electricity and heat generation, figures 4.11(a) (b) display the expected trends of some fundamental parameters. In particular, fig. 4.11(a) illustrates the conditions for heat recovery in terms of thermal output and gas temperature at the heat recovery boiler inlet. A favourable behaviour is exhibited by the latter parameter, mainly because of the stabilizing effect of the recuperated cycle: really, the gas temperature presents slighter variations than those usually occurring for load reduction in a simple cycle gas turbine. This may be intended as a positive aspect because the average temperature of the heat recovery process remains practically unchanged all over the *MGT* operating region. The thermal output substantially follows the trend of the fuel consumption in fig. 4.10(a), as minor decreases are observed for a constant-speed, variable-load operation while the more efficient thermal cycles, obtained when decreasing both mechanical load and shaft speed, result in a reduction of the recoverable heat. In any case, a mechanical load decrease, whichever is the path of the load variation, corresponds to a diminution in thermal output availability.

Conversely, the cycle characteristics produce strong limitations on the values of the typical cogeneration indices (fig. 4.11b). The energy utilization factor is always below the 0.7 level, mainly because of the reduced amount of recoverable heat: really, when operating with fully recuperated cycles, the gas temperature at boiler inlet is rather low and the relative weight of the stack losses (evaluated for a minimum stack temperature of 400K) is enhanced. Similarly, the energy saving ratio, which compares the energy consumption for combined and separated heat and electricity production, achieves fairly acceptable values within a limited area inside the whole *MGT* operating region. However, the best results could be maintained if operating at variable speed, since the fuel energy cost for the mechanical energy production is lower than in the constant speed case.

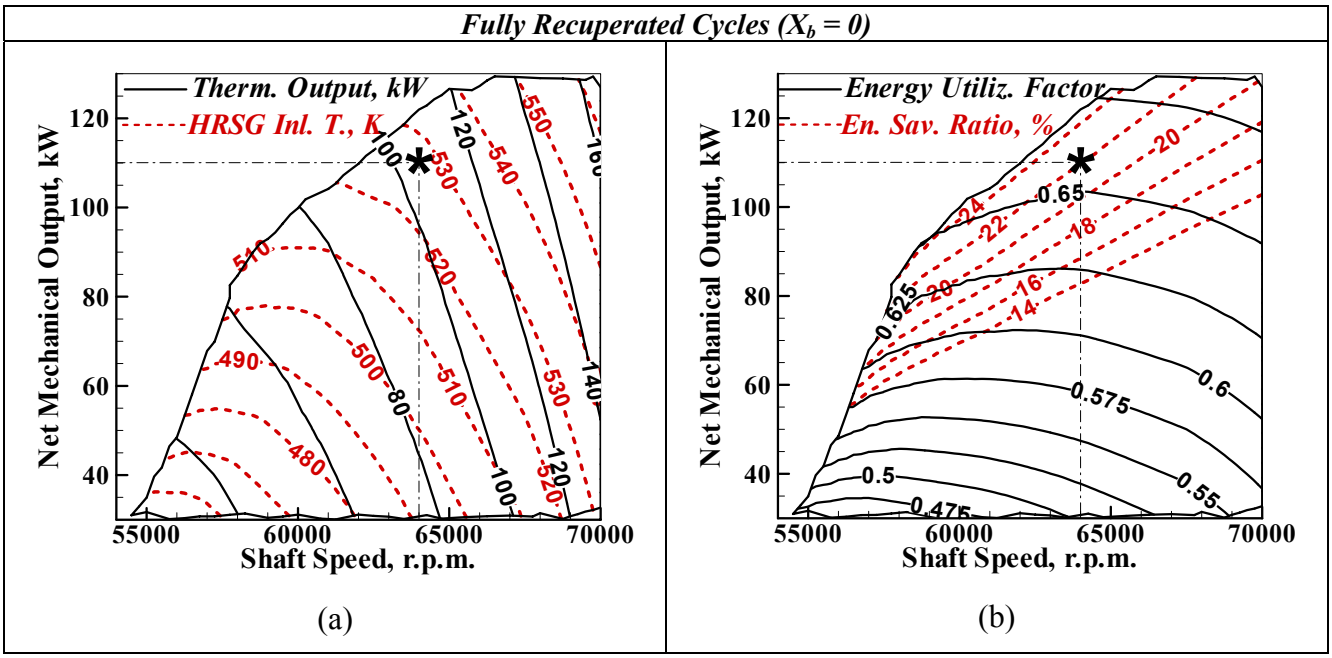

Figure 4.11: Performance Map of the MGT Based Cogenerating Plant.

The last considerations lead to the conclusion that a combined energy conversion system based on the micro-gas turbine should not be considered as an efficient tool for energy saving purpose but it only can be intended as a practical mean for distributed energy production. Following this conclusion, each solution for improving the flexibility of the *MGT* based cogenerating plant can be favourably taken into account.

2) **Variably Recuperated Cycles, Constant-Speed Operation**. Activating the recuperator by pass, i.e., increasing the X_b by-pass ratio, reduces the rate of internal heat transfer. Consequently, each level of mechanical output may be also obtained with less efficient thermal cycles, as demonstrated by the levels of both combustor inlet temperature and efficiency in fig. 4.12. This option can be therefore only considered as an effective tool for adapting the *MGT* response to a wider range of thermal to mechanical output ratios. This assertion is better demonstrated by the following figure 4.13. The X_b increase also produces a rise in the gas temperature at the inlet of the heat recovery device so providing larger amounts of recoverable heat (fig. 4.13a). The gas temperature trend in the same figure also indicates that limitations exist to the application of this method: really, an excess in this values may induce unacceptable thermal stresses to the heat recovery boiler so that large by-pass openings are only allowed for reduced mechanical outputs.

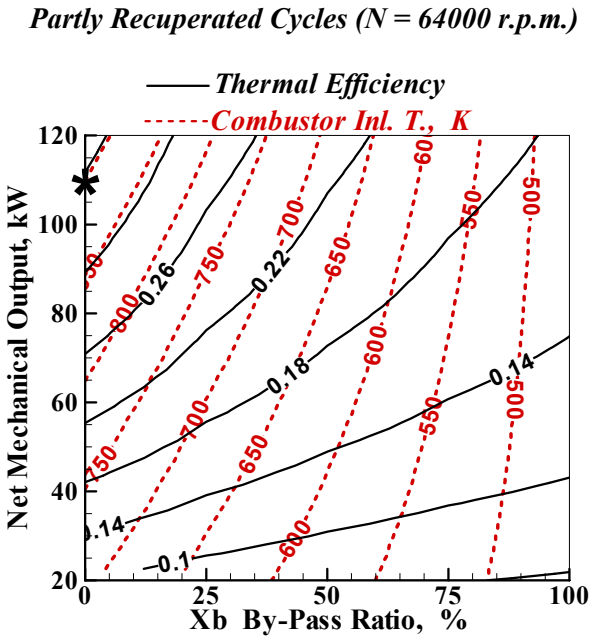

Figure 4.12: Effect of the Recuperator By-Pass on Combustor Inlet Temperature and Thermal Efficiency.

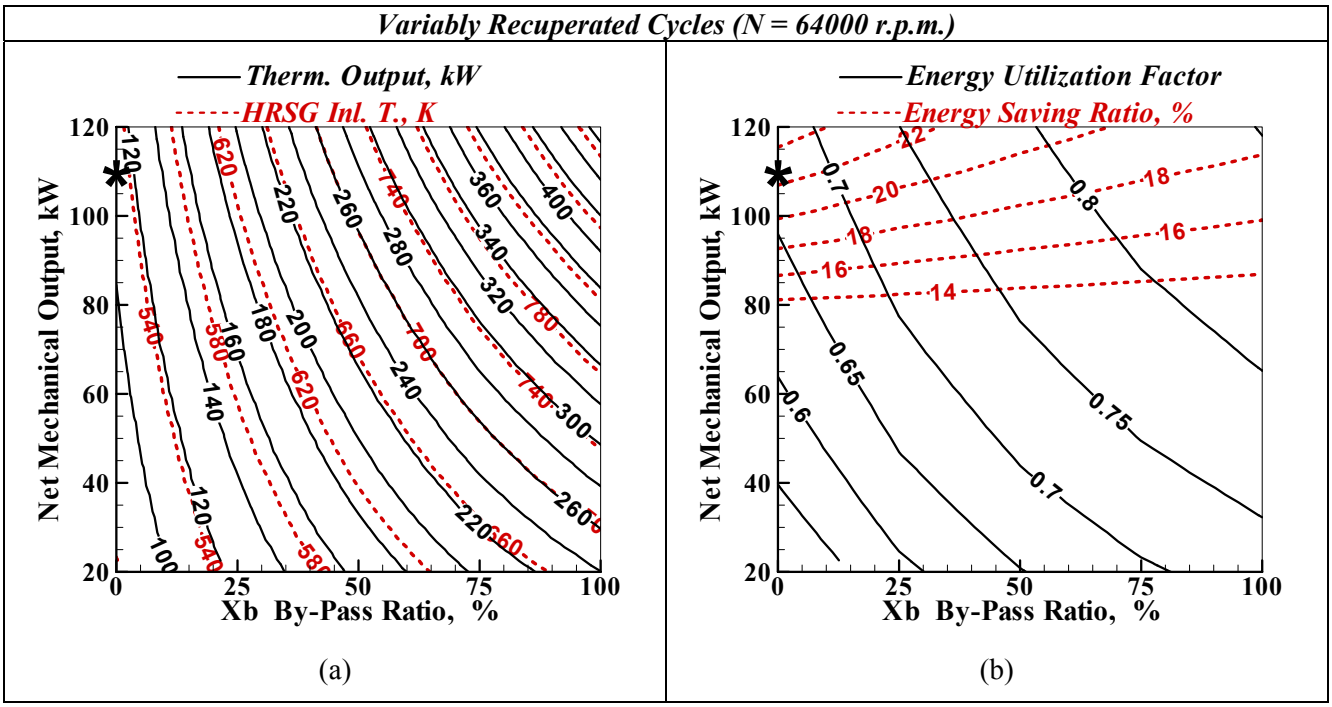

Figure 4.13: Effect of the Recuperator By-Pass on the Cogenerating Performance.

The variable recuperated cycle strategy releases a further degree of freedom to the *MGT* operation and this is of interest specially if a constant speed is imposed by the electrical generator. The curves of thermal output in fig. 4.13a suggest that operating lines different from those detected in the previous figure 4.11 could be chosen, for instance:

- *Constant mechanical output, increasing thermal output with the recuperator by pass*. Fig 4.13(b) suggests that such an operating line would also preserve acceptable levels of the cogenerating performance indices. In particular, the energy utilization factor would achieve better values because of the improvement in the heat recovery conditions. This would almost compensate the decrease in thermal efficiency, so that the energy saving ratio level would undergo only slight decreases along an horizontal line in the (X_b , P) operating plane. Of course, the above named limits on the gas temperature must be taken in to account.
- *Variable mechanical output, constant thermal output, following the iso-contours in fig. 4.13(a)*. This operating line could be easily obtained with moderate by-pass openings, since starting from the base-rating starred point in fig. 4.13(a), a maximum by-pass ratio of 20-25% could be enough to cover the whole range of mechanical output. Along such an operating line, also the HRSG inlet gas temperature would be constant so preserving the average temperature of the heat recovered. Conversely, unfavourable results are observed in terms of the energetic performance, since an almost constant energy utilization factor could be obtained but the energy saving ratio would dramatically drop down. Therefore, choosing this kind of operating line could be only suggested by practical requirements.

3) **Variably Recuperated Cycles, Variable-Speed Operation**. Combining both the strategies discussed above is of interest for overcoming some limitations which result from the application of either the variable speed or the variable by-pass operation. Indeed, looking at the comparison of two operating charts of the micro-gas turbines for fixed values of the Xb ratio (fig. 4.14), the simultaneous employment of both variations could allow preservation of acceptable levels of the energetic indices in a wider range of thermal and mechanical needs.

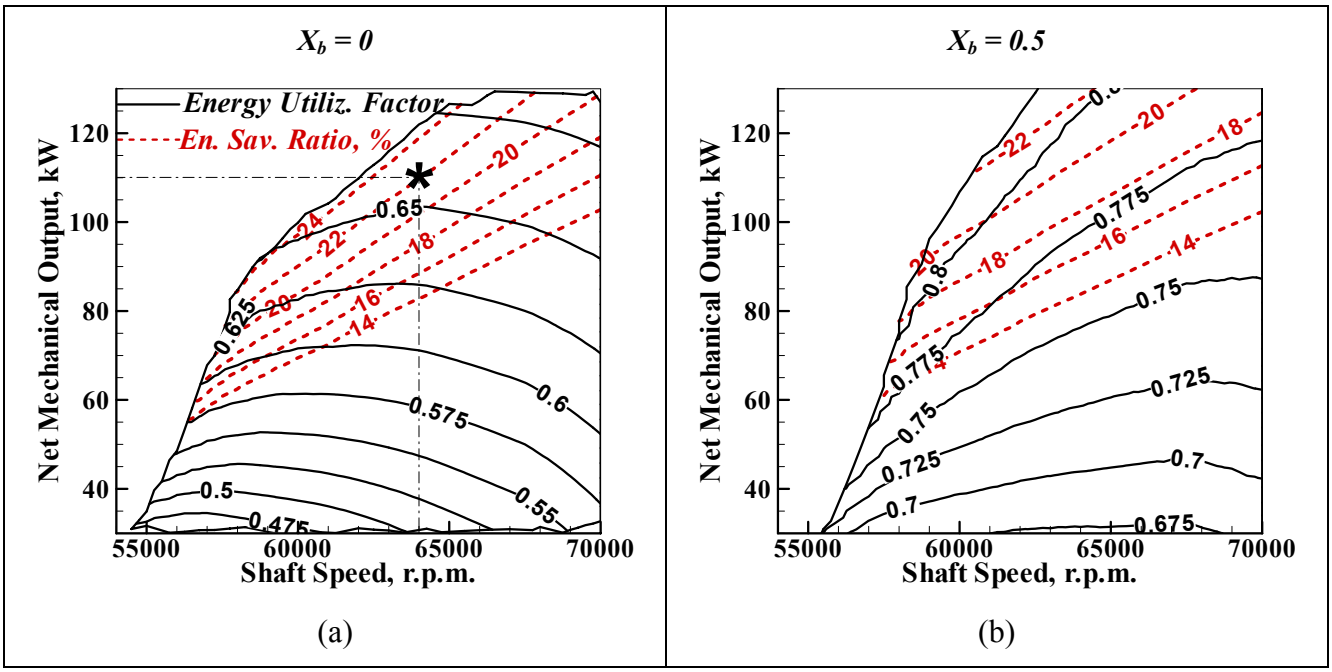

Figure 4.14: Operating Maps of the MGT with Different By-Pass Ratios.

Therefore the simultaneous control of the two independent variables, i.e., the shaft speed and the by-pass ratio could lead to an extension of the operating range with satisfactory energy saving values (fig. 4.15). This figure demonstrates, in particular, that increasing the by-pass ratio while reducing the shaft speed could allow the plant to increase the thermal output (fig. 4.15a) with the same mechanical power but by also keeping the energy saving ratio values within the shaded area of 20% or more (fig. 4.15b). This

represents an interesting difference respect to the constant speed operation with variably recuperated cycles examined in the previous figures 4.13 (a) and (b).

The advantages of this kind of regulation can be also taken for part-load operation (figs. 4.15(c) and (d)) but the extent of the most favourable area is progressively restricted. It is however worth-noting that the operation with the same nominal speed would involve less attractive results in terms of energy saving ratio.

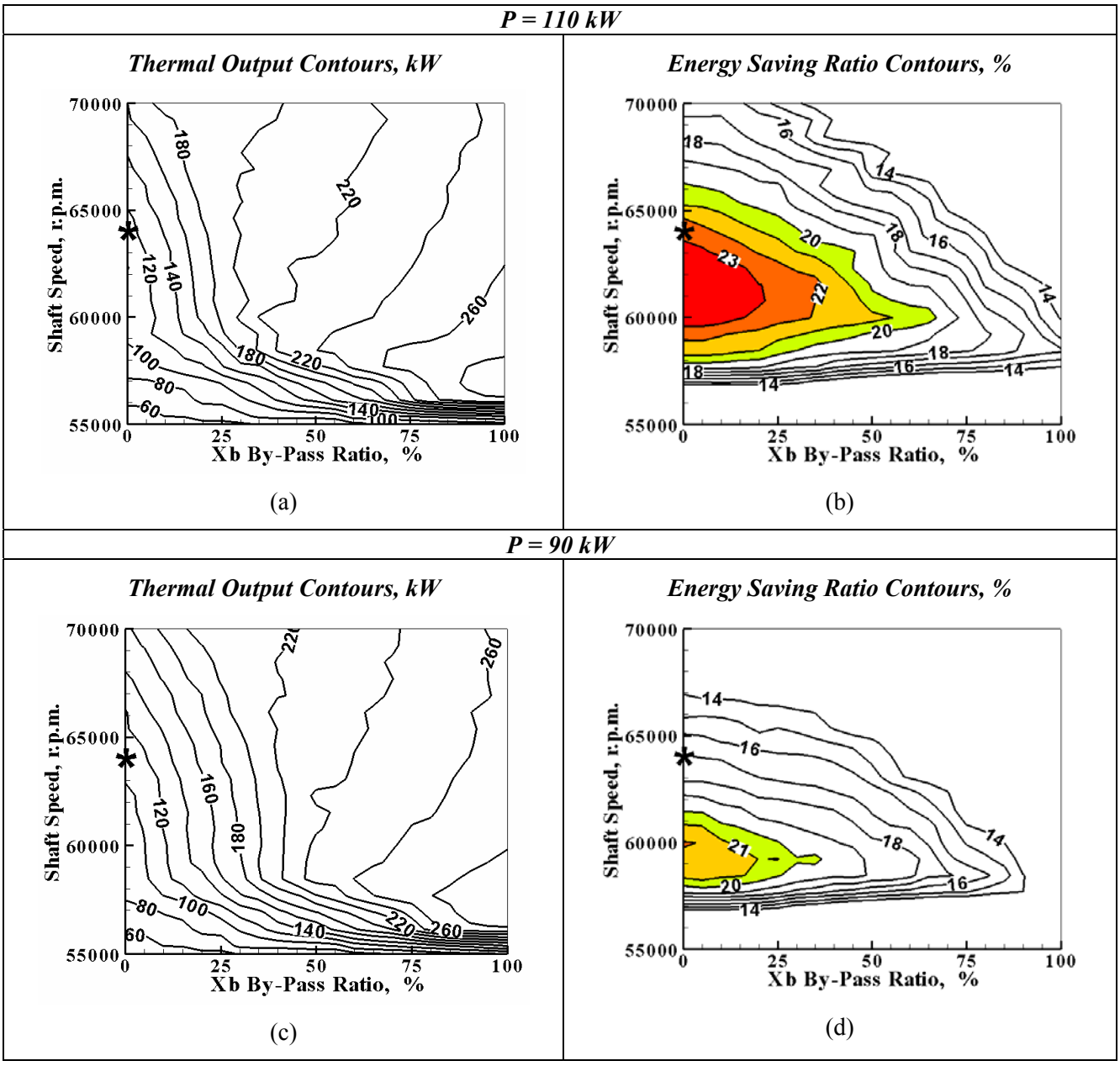

Figure 4.15: Effect of the Simultaneous Variation of Shaft Speed and By-Pass Ratio on the Cogenerating Performance.

5. TRANSIENT ANALYSIS

The completion of the micro-gas turbine performance analysis requires an enhanced study of the MGT operation under transient conditions arising from variations in either the electrical load or in thermal output request. The response characteristic of the system may be really responsible for increases in fuel energy consumption and pollutant production with respect to those expected under steady operation [71-80]. The simulation of a number of transient situations, both of the constant and of the variable MGT shaft speed type, aims at the evaluation of the response characteristic of the most critical components [79]. Compressor stall or unacceptable T.I.T. levels may in fact occur during a sudden variation of the external load, particularly depending on the fuel law specified by the MGT control system.

In this section, which summarizes the contents of the author's paper [74], is presented an extended methodology that employs the component matching analysis by also accounting for the response delay of each rotating or stationary component. The steady-state approach is replaced by a filling-emptying based numerical scheme that better approximates the actual mechanical and fluid-dynamic inertia of the system. The primary attention is obviously focused on the heat exchanger and the combustion chamber, which could exhibit the slowest achievement of the new thermal regimes.

5.1 The Dynamic Model

Figure 5.1 presents a plant schematization based on the definition of four control plenums (i.e., recuperator cold side, combustion chamber, by-pass valve, recuperator hot side), each characterized by its own volume and different inlet and outlet flow areas. The whole system is linked to an intake and exhaust ambient where a constant pressure, temperature and composition are assigned as boundary conditions. Following the filling and emptying technique [71, 74] (zero-dimensional approach), a system of ordinary differential equation (i.e., the mass and energy balance equations) for each component is set. This hypothesis corresponds to neglect propagation effects and allows dropping of the momentum equation:

$$\begin{aligned} \frac{dm}{dt} &= \sum \dot{m}_{in} - \sum \dot{m}_{ex} \\ \frac{d(m\,e)}{dt} &= \sum \dot{m}_{in} h_{in} - \sum \dot{m}_{ex} h_{ex} - \dot{Q}_w + \dot{m}_f h_{0f} \end{aligned} \tag{5.1}$$

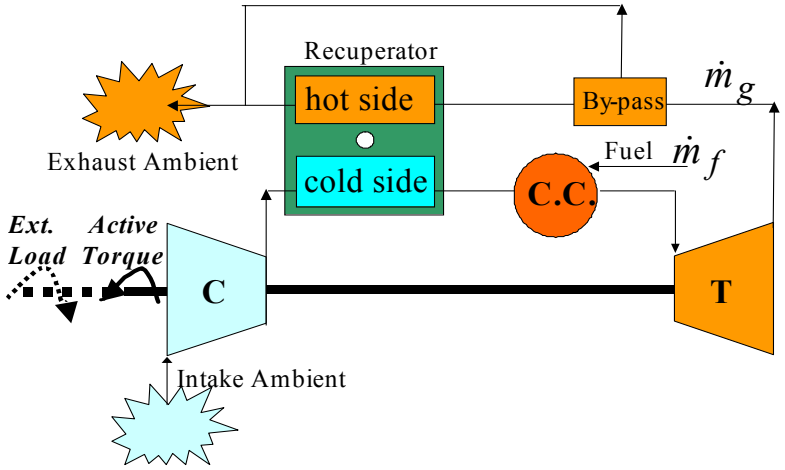

Figure 5.1: Plant Scheme for the Dynamic Model.

The energy equation includes the convective energy flows and the heat transferred through the walls. The last term in the energy equation is active only for combustion chamber volume and represents the rate of chemical energy supplied with the fuel injection. The heat released by the combustion is automatically accounted for, because of the variation in the total internal energy (sum of the sensible and formation energies) during the burning process.

The numerical integration of eqs. (5.1), coupled to the gas state equations [87], allows description of the time evolution of the thermodynamic properties in each control volume. In particular, inlet and outlet flow rates are evaluated as functions of the pressure difference among the adjacent volumes or, alternatively, by accessing the compressor and turbine maps (assumed to be those in fig. 4.1) at the local shaft rotational speed and pressure ratios.

The considerable recuperator volume (of 0.016 m^3 on both cold and hot side) compared with that of the combustion chamber (of 0.0021 m^3) introduces a relevant source of response delay which affects the whole transient process and, in particular, the different rates of change for air and fuel entering the combustor. This will result in significant modifications in the fuel/air equivalence ratio.

The heat transfer rate is computed according to the gas-wall temperature difference and by employing classical correlation for estimating the convective heat transfer coefficient. The equivalent gas temperature responsible for the heat transfer is obtained by averaging the inflow and in-volume temperatures. The time-varying wall temperature accounts for the recuperator thermal inertia and the solution of an additional energy equation is required. The wall temperature trend results from the recuperator matrix heat capacity ($\rho_R\, c_R$ = 3.5x10^6 J/m^3/K), thickness (s_R = 1.0 mm), and heat exchange surface area, (A_R = 51.5 m^2):

$$\frac{dT_{w,R}}{dt} = \frac{\left(\dot{Q}_{in} - \dot{Q}_{ex}\right)}{\left(\rho\, c\, A\, s\right)_R} \tag{5.2}$$

$\left(\dot{Q}_{in} - \dot{Q}_{ex}\right)$ being the heat flux unbalance from the hot to the cold side of the heat exchanger.

At each time step, the instantaneous turbine and compressor mechanical power are finally introduced into the dynamical equilibrium equation of the *MGT* shaft:

$$\frac{dN_{TC}}{dt} = \frac{60^2}{4\pi^2}\frac{\left(P_t - P_c - P_{el}\right)}{I_{TC} N_{TC}} \tag{5.3}$$

According to [71], a value of 3.8x10^{-3} kg m^2 has been selected for the shaft moment of inertia. The transient plant operation can be followed during time as a function of a prescribed external load variation or fuel flow law. In addition, a thermal load variation can be also imposed through the opening/closing of the inlet and outlet passage area of the by-pass control volume.

Regarding the fuel flow rate specification, two different laws are compared in the following:

- The final value of the fuel flow rate is assigned in accordance with the variation in the external load. The dynamical response of the system must therefore follow this pre-determined fuel law, of the exponential decay type with a time-constant of 0.2 s.
- Alternatively, the presence of a “feed-back controller” can be simulated particularly when a constant speed operation of the *MGT* is required. In this case, basing on a simple proportional control law, the time rate of change in fuel flow is a function of the difference between the instantaneous shaft speed and a preset value:

$$\dot{m}_f(t+dt) = \dot{m}_f(t) + \Pi \frac{N_{TC}(t) - N^*_{TC}}{N^*_{TC}} \tag{5.4}$$

The proper value of the Π constant depends on the particular shaft unbalance situation. A more complex *PID* controller could be also set up to reduce both the transient duration and the intensity of undershoots/overshoots of the shaft speed.

5.2 Examples of Transient Development

In accordance with the degrees of freedom identified in the previous section for the MGT base power plant, the transient, off-design process may be induced by either a variation in the electrical load or a change in the thermal output demand. The first one is compensated by adapting the fuel flow rate, while the second one requires also the activation of the recuperator by-pass option.

Regarding to the simple external load variation, we can refer to the typical operating domain which is recalled in fig. 5.2. The points inside the domain must be intended as equilibrium steady states, but each change in either the $\dot{m}_f$ value or in the load constant *K* (defined by eq. 4.10) induces a power unbalance. Therefore, a transient process takes place until the *MGT* power output equals that required by the electrical generator. If a constant speed operation is imposed, the corresponding end points are constrained to lie on a vertical line. Examples are given by points A1 and A2, which refer to a 60% and 40% of nominal output, respectively. If a variable frequency generation is allowed, more favourable part-load conditions can be found, since reducing the rotating speed also leads to a decrease in the fuel flow rate for the same power output, as demonstrated in the previous section. For instance the B2 point in fig. 5.2 has the same level of mechanical output as the A2 point but with a relevantly lower fuel consumption.

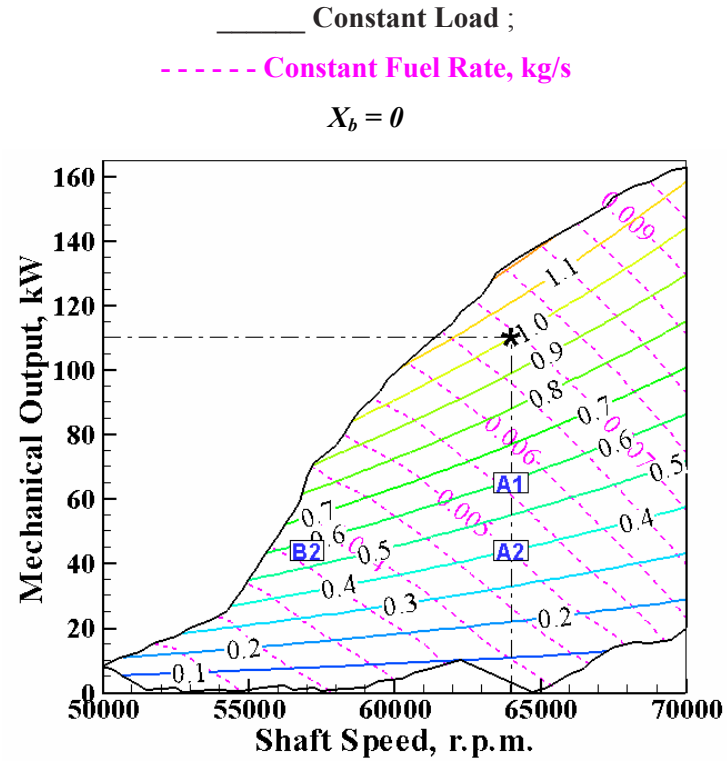

Figure 5.2: Operating MGT Domain with Points for the Transient Simulation.

If the X_b by-pass ratio is directly considered as an independent variable for the *MGT* domains, the effect of the changes in the recuperated cycle can be appreciated (fig. 5.3), mainly in terms of recoverable heat, the latter evaluated for a stack temperature of 403 K. The by-pass option introduces a further degree of freedom which allows the ratio of mechanical to thermal output to be adapted to the actual requirements. Of course, exploiting this concept involves significant variations in the combustor inlet conditions, since the air inlet temperature reduces for increased by-pass levels (as demonstrated by fig. 4.12) and the fuel to air ratio must be increased as to preserve the same firing temperatures.

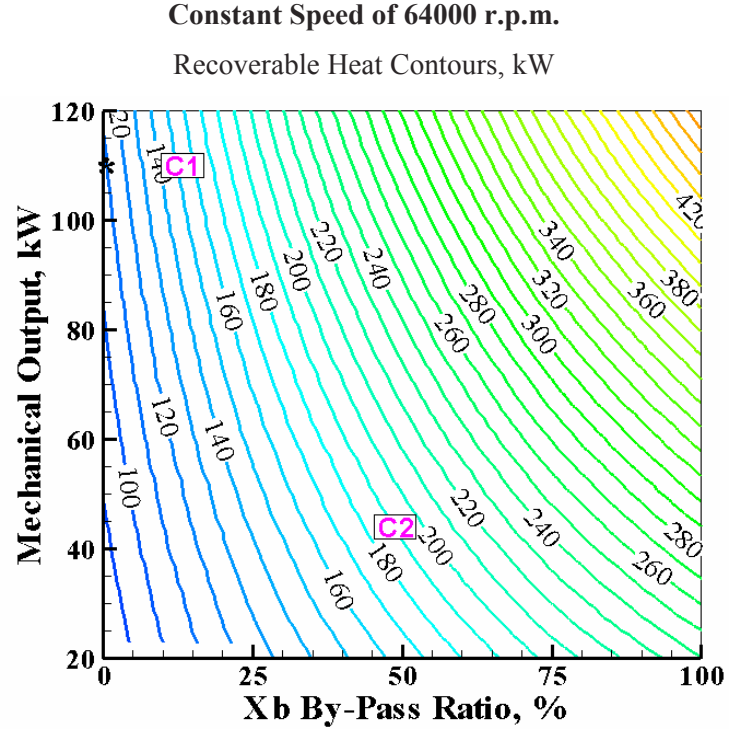

Figure 5.3: Operating Domain with Variably Recuperated Cycles and Points for the Transient Simulation.

Fig. 5.3 recalls the trend of the heat recovery contours when the variably recuperated cycles are adopted and the points C1 and C2 are chosen as typical off-design conditions: the first one corresponds only to an increase in thermal output for constant mechanical output, while the second one implies a 40% load with a simultaneous increase in the thermal energy demand.

Each transient case assumes as a starting point the one designated by "*" in figs. 5.2 and 5.3, and the transient processes are assumed to take place after a sudden variation of the load constant K or of the thermal demand.

Table 5.1 summarizes the performance levels and the values of the operating parameters at the end points of the transient processes.

Table 5.1: Starting and Final Points for the Transient Cases

POINT	P, kW	$\dot{Q}$, kW	N, rpm	K	$\dot{m}_f$, kg/s	*Eqv. Ratio*	$X_{b,\%}$
*	110	108	64000	1.0	.00695	0.142	0
A1	66	95	64000	0.6	.00561	0.111	0
A2	44	88	64000	0.4	.00486	.0992	0
B2	44	50	57000	0.6	.00351	.0984	0
C1	110	153	64000	1.0	.00763	0.155	15.00
C2	44	190	64000	0.4	.00712	0.135	50.00

The curves in fig. 5.4 allow estimation of the different behaviour of the constant-speed, A1 and A2 cases, with respect to the one with variable speed, B2. The first two processes present a significant overspeed, mainly due to the higher values of the final fuel rates, while in the B2 case the rotational speed decreases rather continuously to the final level.

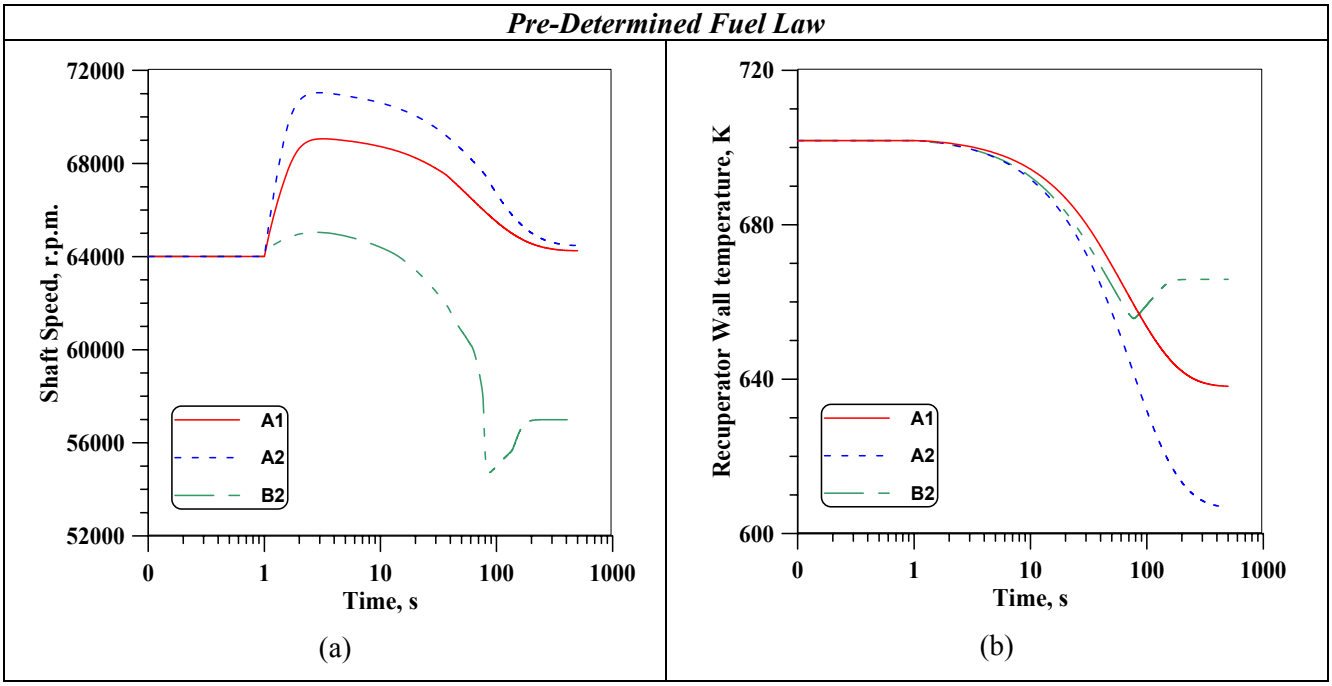

Figure 5.4: Comparison of Different Transient Cases with a Pre-Determined Fuel Law.

The shaft acceleration (fig. 5.4a) in the A1 and A2 cases is also sustained by the increase in the pressure ratio during the unsteady period, which conflicts with the decrease in the firing temperatures and preserves high values of the *MGT* power for a long time interval. The slow changes in the recuperator wall temperatures (fig. 5.4b) govern the regenerative process and the time variations in the combustor inlet temperature. The thermal inertia of the recuperator metal matrix gives reason of the low rate of change in firing temperatures, despite of the sudden decrease in the fuel supply.

In the B2 case, the simultaneous decrease in both pressure ratio and firing temperature would induce more favourable conditions, except for some undesired steep changes. On the other hand the more comprehensive

examination of the transient process B2 (fig. 5.5) evidences that the values of most of the operating variables undergo an excessive decrease respect to the final steady levels. The steep recover of the equilibrium values (fig 5.5a) indicates that conditions close to instability have occurred in some components. This situation is also proved by the superimposition of the transient trace on the compressor map in fig. 5.5(b), which confirms that stall conditions have nearly occurred and the system rather casually reaches the final steady state. A further slight torque unbalance could probably result in a fully instable surging operation.

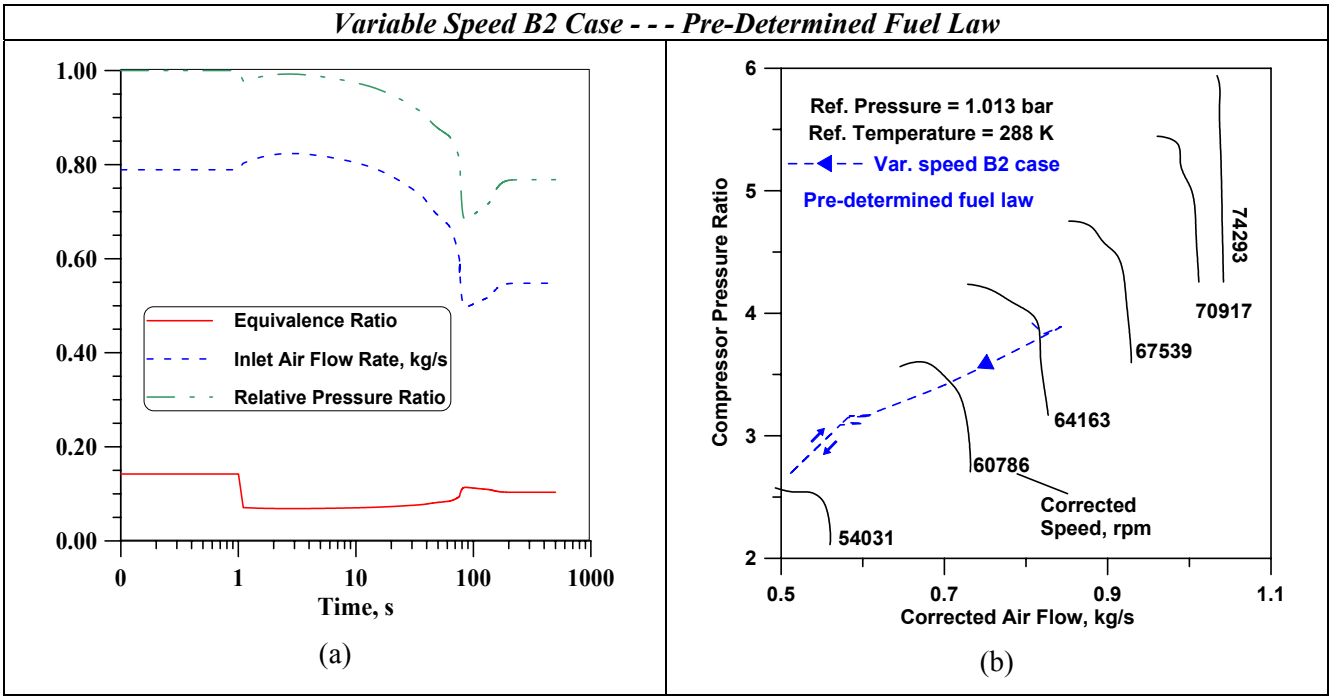

Figure 5.5: Analysis of the Variable Speed Part-Load Case.

The obvious conclusion is that an off-line predetermined law of fuel variation avoids an efficient control of the rotational speed and choking and stall conditions can be expected. The last consideration suggests the introduction of the fuel control law like the one in eq. (5.4).

The next figures 5.6 and 5.7 compare the effects of the pre-determined fuel law, with those resulting from the adoption of the controller in eq. (5.4). The latter are examined under two different hypotheses: the first one assumes that the electrical load variation follows the cubic law in eq. (4.10) (*Variable Pext*), while the second one considers the power required by the electrical generator to be independent of the rotating speed (*Constant Pext* case). This assumption clearly results in more challenging dynamic conditions for the *MTG* group, as demonstrated by the peaks in shaft overspeed in fig. 5.6(b). The fuel laws in fig. 5.6(a) present a smooth behaviour with a decrease of the flow rate below the final level. This produces an efficient control of the rotating speed whose transient is limited within a shorter interval than in the case of the pre-determined fuel variation. In addition, the integral fuel consumption during the transient is clearly reduced. These benefits conflict with some unfavourable trends detected in fig. 5.7(a) in terms of equivalence ratio, say of the actual to stoichiometric fuel/air ratio estimated on the basis of the whole air flow rate entering the combustor. In this sense, a better behaviour is observed when the pre-determined fuel law is imposed. Indeed, an excessive decrease of this parameter would negatively affect the combustion pattern, unless a simultaneous control of the fuel sharing between the main injector and the pilot line is operated in order to prevent the flame quenching.

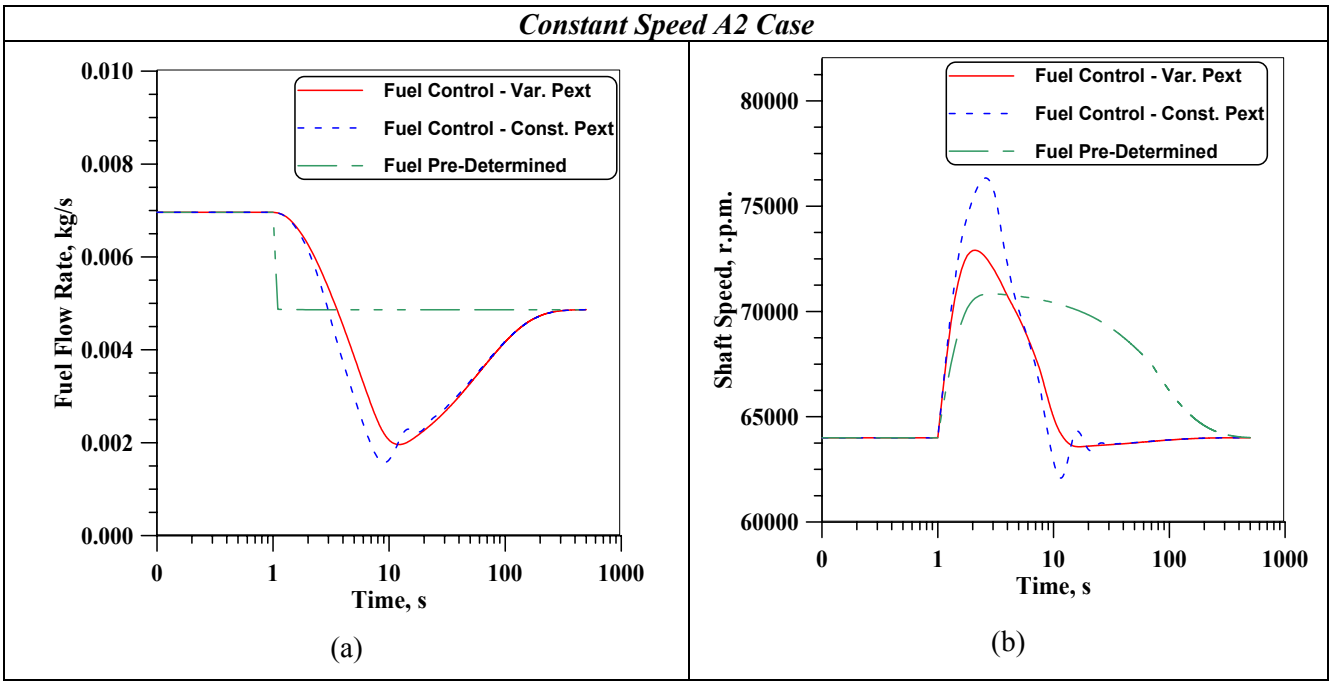

Figure 5.6: Comparison of Different Fuel Supply Laws.

The recuperator wall temperature (fig. 5.7b) undergoes its slow variation almost independently of the fuel laws, and the firing temperature patterns result form the combined effect of these changes and of those in the equivalence ratio. The fuel controller seems to help a faster stabilization of this temperature at the final steady levels. In general, the presence of two distinct phases within the transient process (say, a fast shaft speed transient and a lower unsteady trend of other parameters) is in good agreement with the results of other researchers [71].

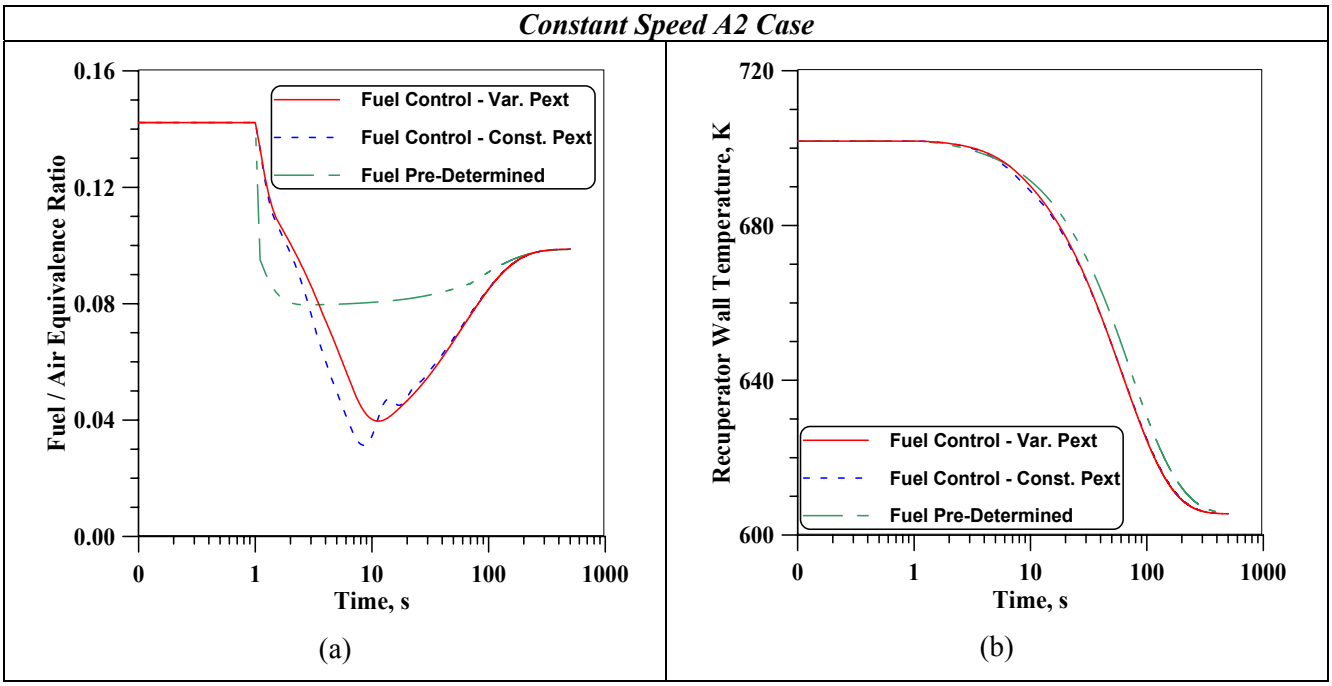

Figure 5.7: Comparison of Different Fuel Supply Laws.

The effectiveness of the fuel control law has been successively checked by comparing the A2 case with the reverse one consisting of a part to full load transient process (fig. 5.8). The initial condition is the A2 point and a sudden change of the *K* constant from the 0.4 to the unit value imposes an increase of the *MGT* power, controlled according to equation (5.4).

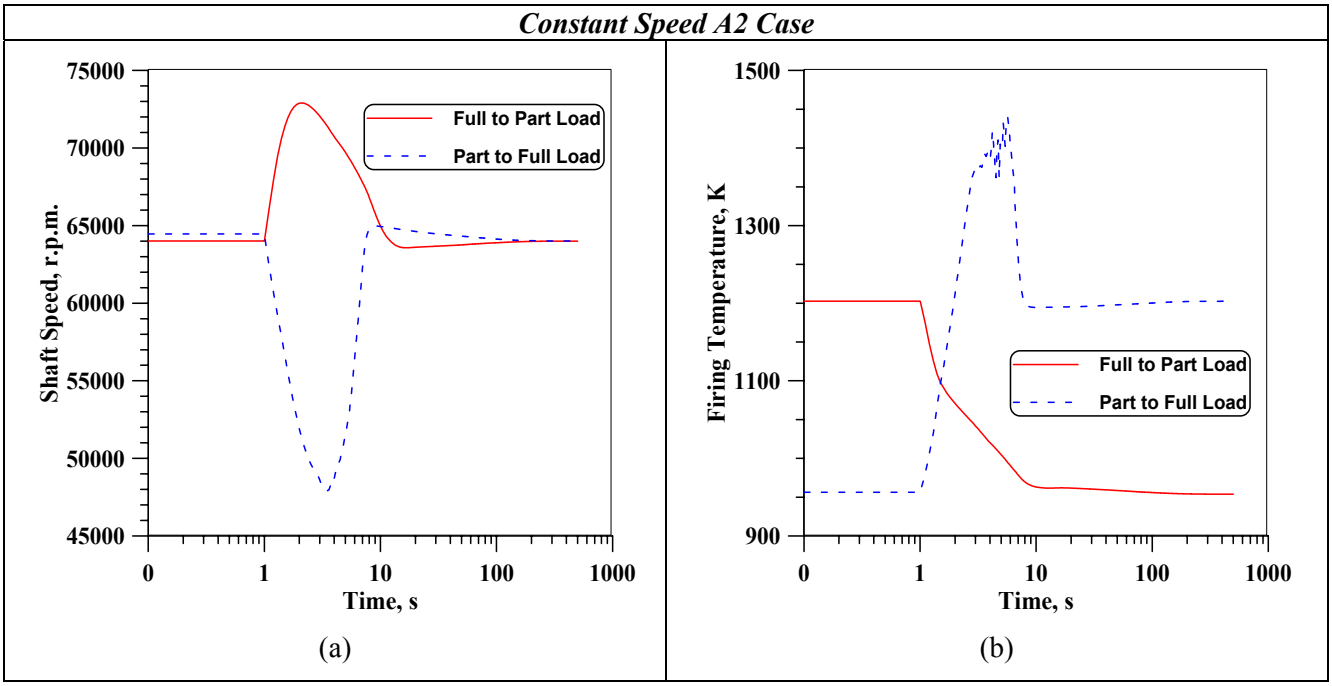

Figure 5.8: Comparison of Opposite Load Transitions.

This process does not completely reflect the one involving the power decrease, since a more dramatic shaft deceleration can be observed in fig. 5.8(a) and the attempt of the system to recover the negative power unbalance is characterized by evident irregularities. These can be explained with the decrease in air mass flow rate which leads to compressor stall at a low compressor speed and it results in undesired peaks in the fuel/air equivalence ratio which are much higher than those expected for a correct combustor operation. The firing temperature itself (fig. 5.8b) rises to excessive levels that are not consistent with a safe activity of the uncooled turbine blades. Concerning the integral fuel consumption in the transient period, the part to full load process involves a significant increase, because the shaft deceleration in fig. 5.8(a) must be quickly recovered by an excess in fuel supply.

The considerations on the compressor transient behaviour are confirmed if tracing the unsteady process on the map in fig. 5.9. The irregularities detected in fig. 5.8b clearly correspond to the operation in the low-speed region, closely to the surge limits. These cases are therefore affected by some uncertainties about the correctness of the approach to the instability conditions in the matching between the compressor and the stationary components. The main source of possible errors can be associated to the employment of steady-state compressor and turbine maps, instead of those actually holding under unsteady conditions.

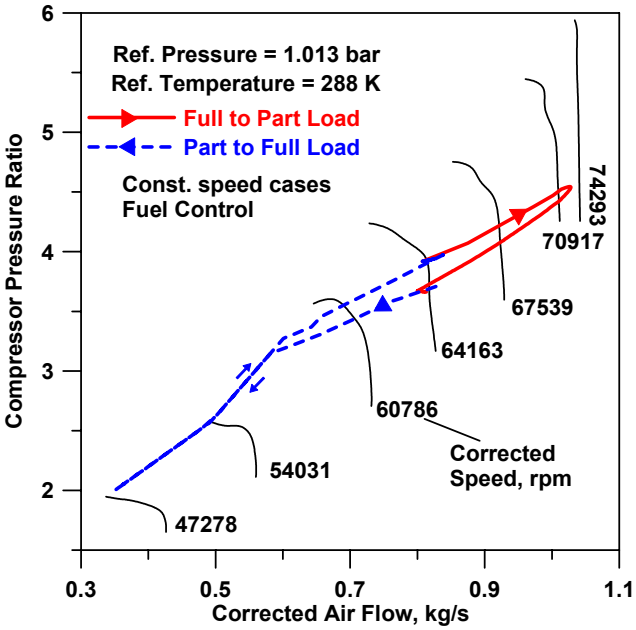

Figure 5.9: Comparison of Opposite Load Transitions.

In order to prevent the system instabilities, a different control law should be chosen or, at least, the Π constant in eq. (5.4) should assume a higher value, so simulating a prompter response of the fuel injection actuator to the controller signals. In paper [74], the authors have shown that the instability risk is reduced if increasing this constant by an order of magnitude but some oscillations in the operating parameters are amplified.

The last examples refer to the variation in the X_b by-pass ratio, in order to follow increased demands of thermal output from the *MGT* based plant. These cases assume as final points those designated with C1 and C2 in fig. 5.3. The first one is at the same level of power output (i.e., K=1.0, the final shaft speed being of 64000 rpm), while the second one represents a part-load condition (K = 0.4), both with raised thermal outputs implying X_b values of 0.15 and 0.5, respectively. The regulation involves therefore both the fuel variation, according to the control law in eq. 4.3, and the by-pass valve opening. The latter occurs in a time of 10 seconds.

The results in figs. 5.10 and 5.11 display the different transient patterns, the C1 case involving slight variations in the operating parameters, the C2 one really being more challenging. The smoother behaviour in all variables in the first transient process is the direct consequence of the unchanged electrical load, so that significant power unbalances are avoided. The C2 process is instead characterized by the typical acceleration in the first transient phase (fig. 5.10b), already detected in the previous examples, followed by the slow achievement of the final steady state. This explains the unexpected increase in gas flow rate through the recuperator in despite of the simultaneous opening of the by-pass valve. The system response is attenuated in terms of decrease in the air temperature at the recuperator outlet (fig. 5.11a), but the related effect is compensated by the provisional decrease in the equivalence ratio, which is helpful for the firing temperature to reach its final value in a reduced time (fig. 5.11b).

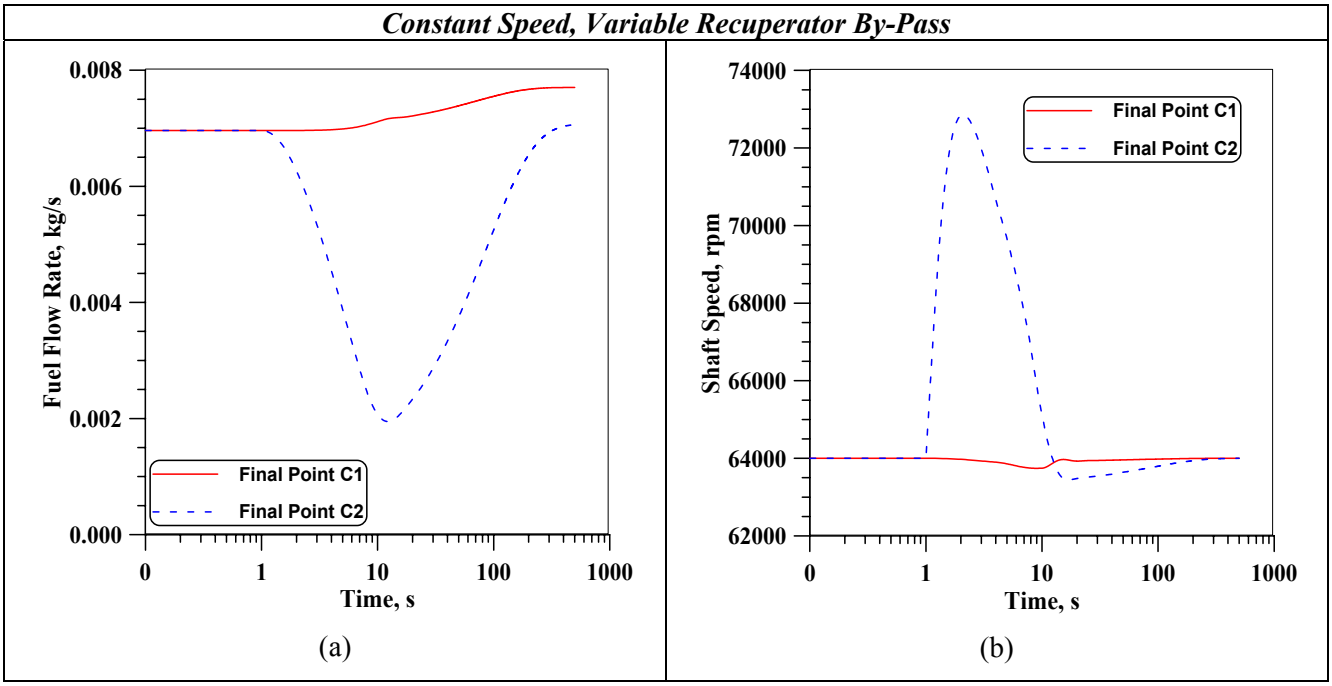

Figure 5.10: Simultaneous Fuel and By-Pass Control. Effect on the Shaft Speed.

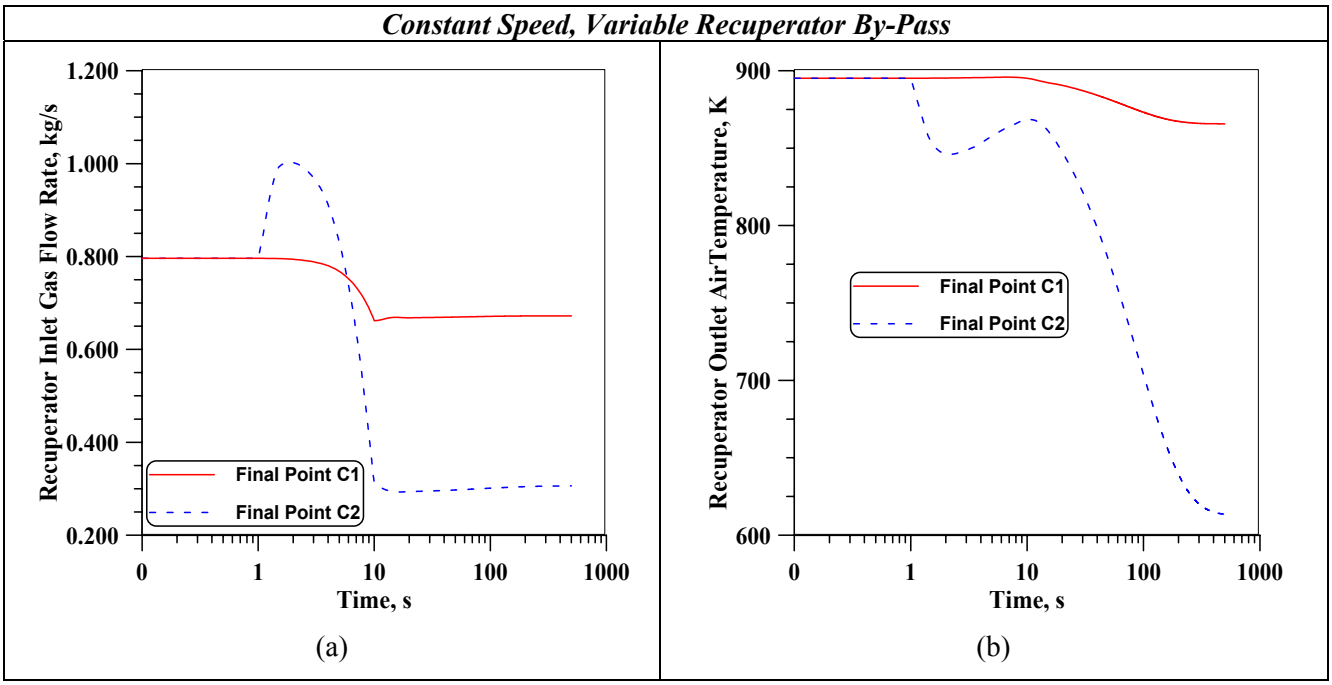

Figure 5.11: Simultaneous Fuel and By-Pass Control. Effect on the Recuperator Behaviour.

It must be recalled again that the last considerations hold under the point of view of the combustor energy balance but they are worthy of more accurate investigations on the actual unsteady behaviour of the combustor. The objective of a prompt response to the augmented thermal requirement appears to be properly fulfilled, because the final decrease in gas flow through the recuperator in fig. 5.10(b) corresponds to a rise in hot gas availability for the heat recovery system, whose unsteady behaviour has not been expressly considered.

CONCLUSION

The wide variety of examples of MGT applications, starting from the isolated power generation systems and proceeding with the cogeneration and tri-generation plants and also including the supplying with alternative fuels, make this subject worthy of an assessment of the methods for performance evaluation.

The consequent purpose of this paper has been to outline the several steps to be generally followed throughout a comprehensive analysis of the MGT based system. Each level of approach contributes to such an assessment, first in terms of cycle analysis and then with a method based on the component matching simulation. The latter is of particular utility when dealing with the problems related to the fulfilment of different external loads. Under this point of view, an interesting role is played by the possibility of operating with variable frequency generators and partly recuperated cycles. Both chances increase the degrees of freedom of the energy conversion system and allow identification of optimal regulation strategies.

The final analysis of the MGT transient phenomena has highlighted the need of setting up proper fuel control laws, in order to prevent the growth of peaks in both firing temperatures and pollutant formation. Such control strategies may be also helpful to avoid out-of-range values for the fuel/air equivalence ratio in the combustor and instable behaviours of the rotating components as well.

All the examples discussed in this paper meet the typical problems which are currently dealt with by many researchers in the *MGT* area, and the attempt to a comprehensive assessment has been pursued through the definition of the above listed methods. In the author's opinion, the integration of these studies with those addressed to the *MGT* combustion may lead to a really exhaustive analysis of the phenomena which characterize the small-scale energy conversion systems.

ACKNOWLEDGMENTS

The researches described in sections 3 to 5 have been carried out also in the course of a cooperation with the *Ansaldo Ricerche* s.p.a. ("Micro-Cogen" research project) that is acknowledged for providing data on the 110kW micro-gas turbine prototype.

The author's researches in the micro-gas turbine field have been supported by the Italian Government within a research project on the dynamics of energy conversion systems (*PRIN 2002*).

Prof. Fabio Bozza is my co-author of all papers describing the methodologies in sections 3 to 5.

Dr. Antonino Pontecorvo and Dr. Fabrizio Reale are acknowledged for contributing to the description of the state of art in section 2 and to some numerical results discussed in sections 3 and 4.

REFERENCES

[1] McDonald, C.F., 1972, Gas Turbine Recuperator Technology Advancements", ASME Paper 72-GT-32.

[2] McDonald, C.F., 1996b, "Heat Exchangers for Very Small Gas Turbines", Intl. Journal of Turbo and Jet Engines, Vol. 13, No. 4, pp. 239-261.

[3] McDonald, C.F., 1997, "Ceramic Heat Exchangers – The Key to High Efficiency in Very Small Gas Turbines", ASME Paper 97-GT-463.

[4] McDonald, C.F., 1999, "Emergence of Recuperated gas Turbines for Power Generation", ASME Paper 99-GT-67.

[5] McDonald, C.F., 2000, "Low Cost Primary Surface Recuperator Concept for Microturbines", ASME Paper 2000-GT-0167.

[6] Maziasz P.J., Swindeman R.W., 2001, "Selecting and Developing Advanced Alloys for Creep-Resistance for Microturbine Recuperator Applications", ASME Paper 2001-GT-0541.

[7] Utriainen E., Sundén B., 2001, "A Comparison of Some Heat Transfer Surfaces for Small Gas Turbine Recuperators", ASME Paper 2001-GT-0474.

[8] Pin B.A., Swindeman R.W., More K.L., Tortorelli P.F., 2001, "Materials Selection for High Temperature (750–1000°C) Metallic Recuperators for Improved Efficiency Microturbines", ASME Paper 2001-GT-0445.

[9] Thompson B.E., Floryan J.M., Nolan R.E., Osgood S.J., 2001, "Enhanced Heat Transfer for Micro-Turbine Recuperators", ASME Paper 2001-GT-0494.

[10] Lagerström G., Xie M., 2002, "High performance & cost effective recuperator for micro-gas turbines", ASME paper 2002-GT-30402.

[11] Takase K., Furukawa H., 2002, "A preliminary study of an inter-cooled and recuperative microgasturbine below 300 kW", ASME paper 2002-GT-30403.

[12] Antoine H., Prieels L., 2002, "The acte spiral recuperator for gas turbine engines", ASME paper 2002-GT-30405.

[13] Proeschel R.A., 2002, "Proe 90™ recuperator for microturbine applications", ASME paper 2002-GT-30406.

[14] Iki N., Furutani H., Takahashi S., 2002, "Conceptual investigation of a small reheat gas turbine system", ASME paper 2003-GT-38473.

[15] Kang K., McKeirnan, 2003, "Annular recuperator development and performance test for 200 kW turbine", ASME Paper, 2003-GT-38522.

[16] Wilson D.G., 2003, "Regenerative heat exchangers for microturbines and an improved type", ASME Paper, 2003-GT-38871.

[17] Traverso A., Zanzarsi, Massardo A.F., 2004, "CHEOPE: A tool for the optimal design of compact recuperators", ASME paper 2004-GT-54114.

[18] Kesseli J., Wolf et. al., 2003, "Micro, industrial, and advanced gas turbines employing recuperators", ASME paper 2003-GT-38938.

[19] Lee H.R., Ellingson W.A., 2000, "Development of Metrological NDE Methods for Microturbine Ceramic Components", ASME Paper 2000-GT-0639.

[20] Newton D., Pollinger J.P., Twait D.J., 2000, "Status of Silicon Nitride Material Properties, Component Fabrication, and Applications for Small Gas Turbines", ASME Paper 2000-GT-0533.

[21] Schenk B., 2000, "Ceramic Turbine Engine Demonstration Project: A Summary Report", ASME Paper 2000-GT-0532.

[22] Schenk B., Tom Strangman T., Opila E.J., Robinson R.C., Fox D.S., Klemm H., Christine Taut C., More K., Torterelli P., 2001, "Oxidation Behavior of Prospective Silicon Nitride Materials for Advanced Microturbine Applications", ASME Paper 2001-GT-0459.

[23] Shi J., Vedula v.R., Holowczak J. et al., 2002, "Preliminary Design of Ceramic Components for the ST5+ Advanced Microturbine Engine", ASME paper 2002-GT-30547.

[24] Lara-Curzio E., Maziasz P.J., Pint B.A., Stewart M., Hamrin D. et al., 2002, "Test facility for screening and evaluating candidate materials for advanced microturbine recuperators", ASME paper 2002-GT-30581.

[25] Schaefer G., Green A.E.S., 2000, "Feedstock Blending in a Continuously Fed Gasifier", ASME Paper 2000-GT-0025.

[26] Buhre B.J.P., Andries J., 2000, "Biomass-Based, Small Scale, Distributed Generation of Electricity and Heat using Integrated Gas Turbine-Fuel Cell" ASME Paper, ASME Paper 2000-GT-0022.

[27] Di Maria F., Desideri U., Bidini G., 2001, "Applicazione di una Microturbina a Gas ad una Discarica di Rifiuti Solidi Urbani", X Convegno Tecnologie e Sistemi energetici complessi, Genova 2001.

[28] Schmitz W., Hein D., 2000, "Concepts for the Production of Biomass Derived Fuel Gases for Gas Turbine Applications," ASME Paper, 2000-GT-0018.

[29] Craig J.D., Purvis C.R., 1999, "A Small Scale Biomass Fuelled Gas Turbine Engine" 1999, ASME Transactions – Journal of Engineering for Gas Turbines and Power, Vol. 121, pp. 64-67.

[30] Fantozzi F., Di Maria F., Desideri U., 2002, "Integrated micro-turbine and rotary-kiln pyrolysis system as a waste to energy solution for a small town in central Italy – cost positioning and global warming assessment –", ASME paper 2002-GT-30652.

[31] Elmegaard, B., Qvale, B., 2002, "Analysis of indirectly fired gas turbine for wet biomass fuels based on commercial micro gas turbine fired data", ASME paper 2002-GT-30016.

[32] Fantozzi F., D'Alessandro B., Desideri U., 2003, "IPCP: Integrated Pyrolysis Combined Plant – An Efficient and Scalable Concept for Gas Turbine Based Energy Conversion from Biomass and Waste", ASME paper 2003-GT-38653.

[33] Bohn D., Lepers J., 2003, "Effects of Biogas Combustion on the Operation Characteristics and Pollutant Emissions of a Micro Gas Turbine", ASME paper 2003-GT-38767.

[34] Chiaramonti D., Riccio G., Martelli F., 2004, "Preliminary Design and Economic Analysis of a Biomass Fed Micro-Gas Turbine Plant for Decentralised Energy Generation in Tuscany", ASME paper 2004-GT-53546.

[35] Fantozzi F., D'Alessandro B., Leonardi D., Desideri U., 2004, "Evaluation of available technologies for chicken manure energy conversion and techno-economic assessment of a case study in Italy", Asme Paper, 2004-GT-54185.

[36] Isomura K., Murayama M., Kawakubo T., 2001, "Feasibility Study of a Gas Turbine at Micro Scale," ASME Paper, 2001-GT-0101.

[37] Spadaccini C.M., Lee J., Lukachko S., Waitz I.A., Mehra A., Zhang X., 2002, "High power density silicon combustion systems for micro gas turbine engines", ASME paper 2002-GT-30082.

[38] Haldeman C.W., O'Brien J.P., Opdyke G et al., 2002, "Low emission combustion turbine experiments with supercritical fuels", ASME paper 2002-GT-30587.

[39] Epstein A.H., 2003, "Millimeter-Scale MEMS Gas Turbine Engines", ASME paper 2003-GT-38866.

[40] Kang S., Johnston J.P., Arima T., 2003, "Micro-Scale Radial-Flow Compressor Impeller Made of Silicon Nitride: Manufacturing and Performance", ASME paper 2003-GT-38933.

[41] Gong, Sirakov, Epstein, Tan, 2004, "Aerothermodynamics of micro-turbomachinery", ASME paper 2004-GT-53877.

[42] Rodgers C., 2000, "25-5 kWe Microturbine Design Aspects," ASME Paper, 2000-GT-0626.

[43] Carno J., et al., 1998, "Micro Gas Turbine for Combined Heat and Power in Distributed Generation", ASME Paper, 98-GT-309.

[44] Rodgers, C., 2001, "Microturbine Cycle Options". ASME Paper 2001-GT-0552.

[45] McDonald C.F. and Rodgers C., 2001, "The Ubiquitous Personal Turbine (PT)... A Power Vision for The 21st Century," ASME Paper, 2001-GT-0100.

[46] Benetta S., Paganucci F., Giglioli R., 2001, "System Description and Test Planning for a Combined Heat and Power (CHP) Plant Composed by a Micro Gas Turbine and an Absorption Chiller/Heatl," ASME Paper, 2001-GT-0102.

[47] Liedtke O., Schulz A., Wittig S., 2002, "Design study of a lean premixed prevaporized counter flow combustor for a micro gas turbine", ASME paper 2002-GT-30074.

[48] Bozzolo M., Brandani M., Traverso A., Massardo A. F., 2002, "Thermoeconomic Analysis of Gas Turbine Plants with Fuel Decarbonisation and Carbon Dioxide Sequestration", ASME paper 2002-GT-30120.

[49] Campanari, Boncompagni, Macchi E., 2002, "Microturbines and trigeneration: optimization strategies and multiple engine configuration effects", ASME paper 2002-GT-30417.

[50] Bozza F., Cameretti M.C., Tuccillo R., 2003, "Adapting the Micro-Gas Turbine Operation to Variable Thermal and Electrical Requirements", ASME paper 2003-GT-38652.

[51] Rodgers C., 2003, "Some effects of size on the performances of small gas turbines", ASME paper 2003-GT-38027.

[52] Benini E., Toffolo A., Lazzaretto, 2003, " Centrifugal Compressor of a 100 kW Microturbine":

a) Part 1 – Experimental and Numerical Investigations on Overall Performance, ASME paper 2003-GT-38152

b) Part 2 – Numerical Study of Impeller-Diffuser Interaction, ASME paper 2003-GT-38153

c) Part 3 – Optimization of Diffuser Apparatus, ASME paper 2003-GT-38154

[53] Campanari, Macchi E., 2003, "Technical and Tariff Scenarios Effect on Microturbine Trigenerative Applications", ASME paper 2003-GT-38275.

[54] Nakagaki T., Ogawa T., Hirata H., Kawamoto K., Ohashi Y., Tanaka K., 2003, "Development of Chemically Recuperated Micro Gas Turbine", Journal of Engineering for Gas Turbines and Power, Volume 125, Number 1 (January 2003).

[55] McDonell V.G., Hack R.L., Lee S.W., Mauzey J.L., et al., 2003, "Experiences with microturbine generator systems installed in the South Coast air quality management district", ASME Paper, 2003-GT-38777.

[56] Gamou S., Ito K., Yokoyama R., 2003, "Parametric study on economic feasibility of microturbine cogeneration systems by an optimization approach", ASME Paper, 2003-GT-38382.

[57] Parente J., Traverso A., Massardo A.F., 2003, "Micro humid air cycle part A: thermodynamic and technical aspects", ASME Paper, 2003-GT-38326.

[58] Parente J., Traverso A., Massardo A.F., 2003, "Micro humid air cycle part B: thermoeconomic analysis", ASME Paper, 2003-GT-38328.

[59] Ibrahim O., Zimmermann P., Hirsch C., Sattelmayer T., Gerhard B., Steinbach C., 2004, "A microturbine operating with variable heat output", ASME paper 2004-GT-53011.

[60] McKee R.J., Gernentz R.S., Hollingsworth J.R. et al., 2004, "A novel centrifugal flow gas turbine design", ASME paper 2004-GT-53063.

[61] Davison C.R., Birk A.M., 2004, "Set up and operational experience with a micro-turbine engine for research and education", ASME paper 2004-GT-53377.

[62] Chiang H.D., Wang C.H., Hsu C., 2004, "Performance testing of a microturbine generator set with twin rotating disk regenerators", ASME paper 2004-GT-53467.

[63] Kang P., Tanaka S., Esashi M., 2004, "Micro Turbocharger on a Single Silicon Rotor", ASME paper 2004-GT-53565.

[64] Sieros G., Kefalakis M., Papailiou K.D., 2004, "Improving turbine performance by use of CFD", ASME paper 2004-GT-53737.

[65] Touchton, et al., 2004, "A novel gas turbine product line for onsite generation and combined heat and power between 400 kWe and 1.6 MWe", ASME paper 2004-GT-54257.

[66] Dodo S., Nakano S., Inoue T., Ichinose M., Yagi M., Tsubouchi K., Yamaguchi K., Hayasaka Y., 2004, "Development of an advanced microturbine system using humid air turbine", ASME paper 2004-GT-54337.

[67] Iki, Takahashi, Furutani, 2004, "Performance of a small reheat gas turbine system as a cogeneration", ASME paper 2004-GT-53837.

[68] González M.A., Padilla R., and Willinger R., 2004, "Combined Heat and Power Technologies: Application Studies of Options Including Micro Gas Turbines", ASME paper 2004-GT-53909.

[69] Ashihara K., Goto A., Guo S., Okamoto H., 2004, "Optimization of Microturbine Aerodynamics Using CFD, Inverse Design and FEM Structural Analysis: 1st Report – Compressor design", ASME paper 2004-GT-53431.

[70] Watanabe H., Okamoto H., Guo S., Goto A., Zangeneh M., 2004, "Optimization of Microturbine Aerodynamics Using CFD, Inverse Design and FEM Structural Analysis: 2nd Report – Turbine Design", ASME paper 2004-GT-53583.

[71] Traverso A., Calzolari, Massardo A.F., 2003, "Transient Analysis and Control System for Advanced Cycles Based on Micro Gas Turbine Technology", ASME paper 2003-GT-38269.

[72] Traverso A., Magistri, Scarpellini, Massardo A.F., 2003, "Demonstration Plant and Expected Performance of an Externally Fired Micro Gas Turbine for Distributed Power Generation" – ASME paper 2003-GT-38268.

[73] Davison, C.R., Birk, A.M., 2004, "Steady state and transient modeling of a micro-turbine with comparison to operating engine", ASME paper 2004-GT-53378.

[74] Bozza, F., and Tuccillo, R., 2004, "Transient Operation Analysis of a Cogenerating Micro-Gas Turbine, ASME paper ESDA-2004-58079.

[75] Zhu, H., and Jackson, G.S., 2001, "Transient Modeling for Assessing Catalytic Combustor Performance in Small Gas Turbine Applications", ASME paper 2001-GT-0520.

[76] Kim, J.H., Song, T.W., Kim, T.S., and Ro, S.T, 2001, "Dynamic Simulation of Full Start-Up Procedure of Heavy Duty Gas Turbines", ASME paper 2001-GT-0017.

[77] Evans, C., Chiras, N., Guillaume, P., and Rees, D., 2001, "Multivariable Modelling of Gas Turbine Dynamics", ASME paper 2001-GT-0018.

[78] Chiras, N., Evans, C., and Rees, D., 2001, "Global Nonlinear Modelling of Gas Turbine Dynamics Using NARMAX", ASME paper 2001-GT-0019.

[79] Arkov, V.Y., Kulikov, G.G., and Breikin, T.V., 2002, "Application of Markov Chains to Identification of Turbine Engine Dynamic Models", ASME paper GT-2002-30038.

[80] Camporeale, S.M., Fortunato, B., and Mastrovito, M., 2002, "A High-Fidelity Real-Time Simulation Code of Gas Turbine Dynamics for Control Applications", ASME paper GT-2002-30039.

[81] Bozza, F., Cameretti, M.C., Tuccillo, R., 2001, "Performance Prediction and Combustion Modelling of Low-CO2 Emission Gas Turbines", *ASME paper* 2001-GT-0066.

[82] Bozza, F., Fontana, G., and Tuccillo R., 1994, "Performance and Emission Levels in Gas Turbine Power Plants," *ASME Transactions – Journ. of Eng. for Gas Turb. and Power*, Vol. 116, pp. 53-62.

[83] Bozza, F., Cameretti, M.C., Marro, A., and Tuccillo, R., 2000, "Performance and emission analysis of a variable load operated gas turbine," in ASME *Advanced Energy Systems*, Vol. 40, pp. 400-415.

[84] Bozza F., Cameretti M.C., Tuccillo R., 2002, "The Employment of Hydrogenated Fuels from Natural Gas Reforming: Gas Turbine and Combustion Analysis" *ASME Jrl of Eng. for Gas Turbines and Power*, Vol. 126, pp. 489-497.

[85] Bozza, F., Senatore, A., and Tuccillo R., 1996, "Thermal Cycle Analysis and Components Aero-Design for Gas Turbine Concept in Low-Range Cogenerating Systems," *ASME Jrl of Eng. for Gas Turbines and Power*, Vol. 118, pp. 792-802.

[86] Cameretti, M.C., and Tuccillo, R., 2004, "Comparing Different Solutions for the Micro-Gas Turbine Combustor", ASME paper GT-2004-53286.

[87] Mc Bride, B.J., and Gordon, S., 1994, "Computer Program for Calculation of Complex Equilibrium Composition and Applications", *NASA RP* 1311, Parts I and II.

[88] Peirs, J., Reynaerts, D., Verplaetsen, F., Norman, F. and Lefever, S., 2003, "Development of a Micro Gas Turbine for Electric Power Generation", proc. of MME 2003, pp. 215-218.